Global and Planetary Change 110 (2013) 195–213

Contents lists available at ScienceDirect

Global and Planetary Change

journal homepage: www.elsevier.com/locate/gloplacha

Modern sedimentation and sediment dispersal pattern on the continental shelf off the Mekong River delta, South China Sea

Witold Szczuciński [a,*], Robert Jagodziński [a], Till J.J. Hanebuth [b], Karl Stattegger [c], Andreas Wetzel [d], Marta Mitręga [a], Daniel Unverricht [c], Phung Van Phach [e]

[a] Institute of Geology, Adam Mickiewicz University in Poznań, Maków Polnych 16, 61-606 Poznań, Poland
[b] MARUM — Center for Marine Environmental Sciences, University of Bremen, Leobener Strasse, 28359 Bremen, Germany
[c] Institute of Geosciences, University of Kiel, Otto-Hahn-Platz 1, 24118 Kiel, Germany
[d] Institute of Geology and Paleontology, Basel University, Bernoullistrasse 32, 4056 Basel, Switzerland
[e] Institute of Marine Geology and Geophysics, Vietnam Academy of Science and Technology, 18 Hoang Quoc Viet Street, Cau Giay District, Hanoi, Viet Nam

ARTICLE INFO

Article history:
Received 7 July 2013
Received in revised form 22 August 2013
Accepted 29 August 2013
Available online 5 September 2013

Keywords:
marine sediments
sediment accumulation rate
sediment geochemistry
clay minerals
Mekong
South China Sea

ABSTRACT

The Mekong River is one of the major suppliers of sediments to the ocean, resulting in the formation of one of the largest river deltas. A major portion of the supplied sediments is accumulated in the subaqueous delta front, which progrades directly off the river mouths and also forms at a distance of more than 200 km westward, next to the Camau Peninsula. This study presents evidence of the existence of a Mekong-fed prodelta further offshore and provides a first quantitative assessment of the modern fluvial-derived sediment dispersal pattern to the subaqueous prodelta, the outer continental shelf and the deep region of the South China Sea. The study is based on 96 surface shelf sediment samples and five short sediment cores, which were analyzed for grain-size composition, carbonate and total organic carbon contents, sedimentary structures (X-ray radiographs), clay mineralogy and bulk geochemistry as well as ^{210}Pb and ^{137}Cs-based sediment accumulation rates. The major sediment types in water depths of 18 m to 112 m include muddy sand, sand, gravelly muddy sand, sandy mud, gravelly sand and mud. The mud is composed mostly of silt fraction, while gravel is primarily composed of shell hash. The sedimentary structures include lamination, cross-stratification, truncation surfaces and burrows of various types. The carbonate content in the sediments varies from 3% close to the Mekong River mouths to 81% further on the shelf. Total organic carbon is from 0.02% in sand to 0.94% in mud. The highest average elemental concentrations are of Si, Ca, Al, Fe, Mg and K. The spatial variability is similar for Al, K and Ti, as well as for Ca and Sr, suggesting the common presence in phyllosilicates and calcium carbonate minerals, respectively. The most common clay mineral is illite followed by smectite, kaolinite and chlorite. The spatial distribution of clay minerals suggests that they are primarily derived from the Mekong River, except in the northeastern region. The sediment accumulation rates in the mud-rich portion of the study area are in the range of 0.1 to 1.5 cm yr^{-1}. According to these results, the shelf environment is divided into three zones. Westward and southward from the Camau Peninsula, the subaqueous prodelta (water depth < 32 m) appears as a mud-dominated, organic-rich, high-accumulation (up to 1.5 cm yr^{-1}) zone. South of the river mouths, a wide zone is dominated by terrigenous sands, which most likely represent the sink for river-supplied bedload sediments. The third and most offshore located zone of moderate-accumulation (0.3–0.4 cm yr^{-1}) is dominated by muddy sands that are rich in biogenic carbonate. Evidence of redeposition, event deposition and changing sedimentary conditions is found in each of these zones reflecting the combined effects of tides, the changing monsoonal current and wind regimes and episodic tropical storms. The sediment budget calculation reveals that the subaqueous delta front stores approximately 50% of the fine-grained sediments supplied by the Mekong River. Roughly one-fourth of the sediments are retained in the subaerial region of the delta (including the Tonle Sap Lake), and approximately 25% accumulates on the shelf around the Camau Peninsula, primarily in the form of prodelta deposits. These results do not suggest a significant export of fine-grained sediments into the deep region of the South China Sea.

1. Introduction

Global sediment fluxes from the continents to the adjacent coastal seas and deep oceans originate primarily from river discharge (Milliman and Meade, 1983; Milliman and Syvitski, 1992; Hay, 1998). Southeastern and eastern Asia is the area with the largest fluvial

* Corresponding author at: Institute of Geology, Adam Mickiewicz University in Poznań, Maków Polnych 16, 61-606 Poznań, Poland. Tel.: +48 618296025; fax: +48 618296001.
E-mail address: witek@amu.edu.pl (W. Szczuciński).

0921-8181/$ – see front matter © 2013 Elsevier B.V. All rights reserved.
http://dx.doi.org/10.1016/j.gloplacha.2013.08.019

sediment supply to the world's ocean. The Ganges, Brahmaputra, Huang He, Yangtze, Irrawaddy and Mekong Rivers are among the top ten in terms of worldwide sediment discharge, accounting for ~30% of the global fluvial sediment flux to the sea (Milliman and Syvitski, 1992). This enormous riverine sediment delivery has a strong influence on many important global and regional processes, including global biogeochemical transformations, water-quality changes and coastal erosion (e.g., Conley, 1997; Syvitski and Milliman, 2007). However, quantitative measurements of sediment discharge have been carried out on less than 10% of the rivers worldwide (Syvitski et al., 2005). Therefore, most of the fluvial sediment load estimates are available from modeling studies alone and with limited accuracy (e.g., Syvitski et al., 2005; Cohen et al., 2013). Less is known of the fate of fluvial sediments that reach the sea because they may be stored in coastal, deltaic or estuarine systems and/or be dispersed through various processes over the continental shelf and slope (e.g., Wetzel, 1993; Goodbred and Kuehl, 1999; Sommerfield et al., 2007; Walsh and Nittrouer, 2009; Hanebuth et al., 2011). Quantitative assessment of the dispersal pattern of fluvial-derived sediments is not a trivial task but is crucially required because the future fate of the densely populated mega-deltas depends largely on their overall sediment budget (Syvitski et al., 2009). Furthermore, the shallow continental shelf areas are increasingly used for various purposes (e.g., transportation, aquaculture, mining, fishery and tourism) that depend on or have an effect on the seabed sediment composition and accumulation pattern.

The Mekong is one of the world's major rivers: it is the 12th-longest river in the world and drains an area of 795,000 km^2 from the Tibetan Plateau down to the coast of the South China Sea. The delivery of sediments during the past 8000 years (Nguyen et al., 2000; Tamura et al., 2009; Nguyen et al., 2010; Hanebuth et al., 2012) resulted in the formation of the third largest delta plain worldwide (62,500 km^2; Coleman and Roberts, 1989). As the delta prograded its character changed from a tide-dominated to a tide-and-wave-dominated system (Ta et al., 2002a,b). This delta is divided into a 150-km wide subaerial plain and a subaqueous portion. The later is composed of two major delta fronts along the delta's coast but located greater than 200 km apart from each other as preliminary noted by Ta et al. (2005) and recently documented by Xue et al. (2010, in press) and Unverricht et al. (2013–this issue). One delta front is located next to the modern Mekong River mouths and progrades seaward. The other front forms near the Camau Peninsula at the most southwestern spit of the Mekong Delta (Fig. 1). Liu et al. (2009) and Xue et al. (2010) suggested that this subaqueous delta might store major amounts of Mekong River discharge. However, precise volume estimates have not been assessed thus far. Moreover, the dispersal pattern and the amounts of sediments transported further offshore to the subaqueous prodelta, the open continental shelf and the deep region of the South China Sea are still unknown. In the literature, speculations on the final fate of the Mekong River sediments are somewhat controversial. It has been suggested that the Mekong River delivers a considerable amount of sediment to the deep South China Sea (e.g., Liu et al., 2004; Fu et al., 2011), whereas the delta-based studies suggested that most of the sediment is transported in the opposite (i.e., westward) direction toward the Gulf of Thailand (Nguyen et al., 2000; Xue et al., 2010; Unverricht et al., 2013–this issue). The latter finding is supported by relict deposits or a notably thin Holocene drape that suggests zero to rather low fluvial input to wide areas of the southern Vietnamese continental shelf (Emery, 1968; Hanebuth and Stattegger, 2004; Jagodziński, 2005; Schimanski and Stattegger, 2005). Knowledge of the modern fate of the Mekong-derived sediments is also important for the estimation of the expected near-future changes in the discharge related to extensive damming projects (e.g., Kummu et al., 2010; Wang et al., 2011).

The current study focuses on an area located approximately 20 km to 120 km (i.e., just seaward of the subaqueous delta front) off the shorelines of the Mekong River delta and extending 450 km west and 200 km east off the Mekong River mouths (Fig. 1). Previous studies on sediments in this area were largely limited to a few sampling points and addressed the sediment dynamics, sedimentary properties, mineralogy or geochemistry (e.g., Emery and Nino, 1963; Chen, 1978; Anikiev et al., 1986, 2001, 2004; Kubicki, 2008; Unverricht et al., in press), focusing primarily on the area located next to the Mekong River mouths (Fig. 1). However, offshore of the subaqueous delta front, the sediment distribution pattern is not well known, and no assessments of modern sediment accumulation rates are available.

Therefore, the current study extends the existing studies of continental shelf sediments adjacent to the Mekong River delta. A total of 96 sediment samples were collected at 18 m to 50 m of the modern water depth and were supplemented by additional samples from the deeper shelf (down to 112 m; Fig. 1). The major objectives of this study are: (1) to present a comprehensive surface-sediment data set based on sedimentary properties, clay mineralogy and bulk geochemistry for the study area; (2) to determine the dispersal pattern of Mekong River sediments on the adjacent continental shelf and to evaluate which processes dominate the modern sedimentation; and (3) to provide a modern (past century) sediment budget estimate for the successive depositional environments of the lower Mekong River system including the delta plain, subaqueous delta and adjacent continental shelf.

2. Regional setting

The study area is located from 104.2° to 109.5°E and 8.1° to 11.1°N (Fig. 1). This area covers the transition between the narrow shelf off central Vietnam in the northwest and the wide Sunda Shelf and Gulf of Thailand in the southern and western directions (Fig. 1). During the last glacial maximum, this shelf widely emerged because the sea level was lowered by approximately 123 m (Hanebuth et al., 2009). The open shelf off the Mekong River is covered by sandy relict and palimpsest deposits (Anikiev et al., 2001; Jagodziński, 2005; Schimanski and Stattegger, 2005; Kubicki, 2008).

The major sediment supply comes from the Mekong River, which splits at the apex of its large delta plain into two main distributaries, the Bassac (Hau River) and the Mekong (Tien River), which subsequently divide into the two branches of the Bassac and six branches of the Mekong before entering the South China Sea. The subaerial delta progrades primarily in the western direction (Nguyen et al., 2000), where the prominent Camau Peninsula has developed (Fig. 1). In front of the main Mekong River mouths and around the Camau Peninsula, a subaqueous delta front extends greater than 20 km offshore and is composed of up to 20-m-thick sediments of topset–foreset–bottomset architecture (Gagliano and McIntire, 1968; Xue et al., 2010; Unverricht et al., 2013–this issue). Sediments of the subaqueous delta front consist of well-sorted fine sands in the Mekong River mouths area with a southwestward fining gradient. Around the Camau Peninsula and in the Gulf of Thailand, these subaqueous delta deposits are composed of well-sorted fine silts (Unverricht et al., 2013–this issue; Xue et al., in press).

The general sediment distribution pattern offshore of the subaqueous delta front was documented based on a few samples by Emery and Nino (1963), Nguyen (1996), Hieu (1998), and Wetzel et al. (2010) and limited mineralogical data from Chen (1978). The only area that is relatively well studied using sedimentological and geochemical approaches is located next to the Mekong River mouths. In that area, sands and relict deposits were primarily documented (Astakhov et al., 1989; Anikiev et al., 2004; Cenci and Martin, 2004) and subaqueous sand dunes are common further east (Kubicki, 2008; Bui et al., 2009).

The study area is affected by the Southeast Asian Monsoon, which drives the seasonality of the river discharge. The water discharge of the Mekong River is estimated as 470 km^3 yr^{-1} (Milliman and Meade, 1983) but varies significantly with the particular monsoon season. A total of 85% of the annual water discharge occurs during the rainy

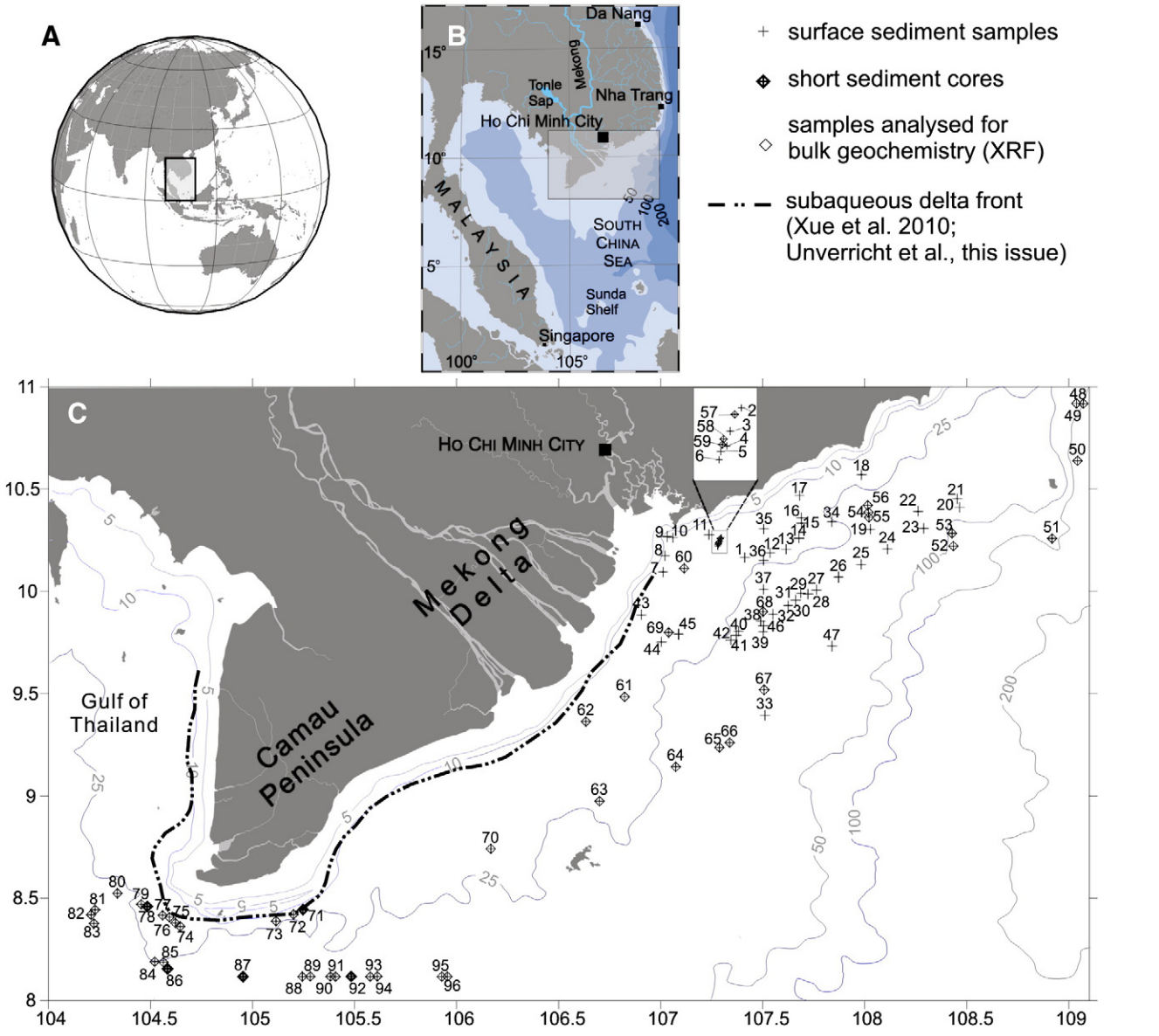

Fig. 1. Study area; A) and B) represent the location of the study area in global and regional contexts, respectively; C) Location of sampling stations. The delta front of the subaqueous delta is marked after Xue et al. (2010) and Unverricht et al. (2013–this issue).

season, between May and October (Le et al., 2007). The suspended load of the Mekong River fluctuates seasonally as well. On average, the load amounts to approximately 160×10^9 kg yr^{-1}, as measured about 800 km upstream from the river mouth (Milliman and Syvitski, 1992), but such estimates vary significantly relative to measurement techniques, inter-annual fluctuations and recent dam constructions (Wang et al., 2011). The suspended sediment in the lower reaches of the Mekong River is mostly composed of fine silt with about 15% clay (Wolanski et al., 1996). The suspended sediment distribution across the shelf was recently studied over one inter-monsoonal season by Unverricht et al. (in press). This study proved that the highest sediment concentrations are found next to the river mouths and around the Camau Peninsula (Fig. 1), where sediments are continuously resuspended by tide-induced currents, even during the calm season and neap tides.

In the winter monsoon season from November to early March, the winds blow mainly from the northeastern and east directions, and southwestern winds prevail during the summer monsoon (Unverricht et al., in press). The wave climate differs significantly between the seasons and within local areas. In the river mouth area, waves higher than 1 m may occur at the coastline year-round (Tamura et al., 2010).

The shelf current system is also controlled by the monsoonal system. The coastal currents follow a southwestern direction during the winter monsoon but a northeastern direction during the summer season. According to numerical models, the current velocities inside the sheltered Gulf of Thailand are much lower than those in the open South China Sea during both monsoon seasons (Wendong et al., 1998; Hordoir et al., 2006; Xue et al., 2012). The study area is also affected by tropical storms in November and December. During the past 50 years, more than 30 severe storms with typical passage duration of 3 to 5 days have hit the southern Vietnamese coast, resulting in rapid coastal erosion (Nguyen, 2012). The maximum wind speed during such storm events is between 40 km h^{-1} and 180 km h^{-1} (UNISYS, 2013).

The Mekong River delta is affected by tides of a mixed diurnal and semi-diurnal character (Fang et al., 1999; Zu et al., 2008; Nguyen,

2012). Along the delta coast exposed toward the South China Sea, a meso-tidal regime prevails with spring tide amplitudes decreasing westward from up to 3.8 m in the east to approximately 2 m near the spit of the Camau Peninsula (Nguyen, 2012). In the Gulf of Thailand, a micro-tidal diurnal system occurs with tidal ranges between 0.5 and 1.0 m.

3. Materials and methods

3.1. Sampling

The sample material was collected during the VG-5 and VG-9 cruises with the R/V *Nghien Cuu Bien* in May 2004 and April 2005 and the R/V *Sonne* cruise SO 187/Leg 3 in April–May 2006 (Wiesner et al., 2006). In total, 96 surface sediment samples and 5 short sediment cores from water depths of 18 m to 112 m were investigated (Fig. 1, Appendix 1 in the Supplementary online material). The material was sampled from the uppermost 5 cm. Samples 1 through 47 were collected with a grab sampler and the other samples were taken with a giant box corer with a surface area of 50 cm^2. All of the surface samples were analyzed for grain size and carbonate content, 92 samples for total carbon and total organic carbon content, 73 for clay minerals and 47 for bulk geochemistry. The sediments retrieved with box corer were sub-sampled for X-ray radiographic imaging (the uppermost 25 cm of the core, if available), and sub-cores of 10 cm in diameter were taken at five sites for sediment accumulation rate assessment and were analyzed for downcore variations in grain size and carbonate content.

3.2. Sedimentary properties

All samples were described and photographed directly on board. The surface relief and sedimentary structure of the deposits recovered with the giant box corer were documented as well. The surface samples (N = 96) and samples from each of the five short cores (N = 25) were wet-sieved at 0.063 mm, and the sand and gravel fractions were separated by dry sieving into six grain-size fractions using mesh sizes of 2, 1, 0.5, 0.25 and 0.125 mm. The clay-fraction content was assessed via grain-size separation by centrifuge settling together with preparation for clay-mineral analysis. The sediments were classified according to their grain-size distribution using Folk's (1954) simplified scheme.

Digital X-ray radiographs were obtained from 0.5 × 10 × 25 cm slabs taken directly from the front side of an opened giant box core (Fig. 2C), and X-ray radiographs (negatives) were acquired at the Prüner Gang Medical Center (Kiel, Germany). The X-ray radiographs were used to detect internal sedimentary structures or unconformities often not visible in the fresh cores.

3.3. Clay minerals

In this study, the term "clay minerals" refers to the four major phyllosilicate minerals of smectite, illite, kaolinite and chlorite that appear in the clay grain-size fraction (<2 μm). Compositional differences within each of these groups were not further considered. The methodological approach followed was that applied by Jagodziński (2005) for surface sediments of the nearby Vietnam and Sunda shelves. The clay fraction of the 73 samples (Appendix 1 in the Supplementary online material) was separated by centrifuge settling and oriented by wet-smearing on glass slides. The X-ray diffraction (XRD) analyses were run on a ARL X'tra (theta–theta goniometer; Cu Kα radiation; Peltier cooled Si(Li) solid-state detector) from Thermo Electron (Institute of Geology, Adam Mickiewicz University in Poznań, Poland). Three XRD runs were performed for each sample, one for the air-dried sample, a second after treatment with glycol and a third after heating at 550 °C. The contents of each mineral group were calculated via semi-quantitative analysis of the obtained diffractograms, following the method of Biscaye (1965) and using the MacDiff 4.2.5 software set up by Petschik (2000). The relative clay mineral abundances are given as a percent of their sum. According to Biscaye (1965), the accuracy of this method is ±5–10%, and the presented relative mineral abundances are rounded to full numbers.

3.4. Sediment geochemistry

The bulk sediment samples were dried and manually grounded for the analyses of carbonate content, total organic carbon content (TOC), and the elemental concentrations of 12 elements. The bulk carbonate content was determined for all surface samples (N = 96) and short cores (N = 43) using the carbonate bomb technique of Müller and Gastner (1971) with a reproducibility of ±1%.

The contents of TOC were measured for 92 samples using a Leco CS-300 element analyzer (Bremen University, Germany). The samples were treated with 12.5% HCl to remove inorganic carbon prior to the measurement of TOC. The analytical precision of the analysis is ±3%.

The bulk concentrations of 12 elements (Al, Br, Ca, Fe, K, Mg, Mn, P, S, Si, Sr and Ti) were determined for 47 samples (Fig. 1) via energy-dispersive polarization X-ray fluorescence (EDP-XRF) spectrometry using a Spectro Xepos instrument at Bremen University (Germany). The instrument was controlled using Spectro X-Lab Pro software, version 2.4, with the so-called TurboQuant method. A measuring time of 100 s per target and sample was used for analysis. Analytical quality was assessed by daily analyses of a pressed pellet of MAG-1 standard reference material (Govindaraju, 1994).

3.5. Sediment accumulation rates

Sediment accumulation rates (SARs) for the past one hundred years (approximately) were assessed through ^{210}Pb and ^{137}Cs analyses. The activities of both isotopes were measured by gamma spectroscopy using a Canberra GX2520 high-purity coaxial germanium detector with a remote detector chamber option (RDC-6 in.) housed in the Institute of Geology of the Adam Mickiewicz University in Poznań (Poland). The efficiencies for the measured geometries were determined using LabSOCS (Laboratory Sourceless Calibration Software) code which applies all corrections for sample geometry, matrix, and container type. Samples were taken from five sediment cores in 5-cm thick intervals. The samples were dried, grounded and packed into sealed containers for further measurements, which took place several weeks later. Measurement of 20 g of dry sediment lasted for 24 h. The obtained activities were decay-corrected to the date of sampling, and the results are reported within a two-sigma standard deviation uncertainty range.

The SARs were calculated from the decrease of excess ^{210}Pb activities with sediment depth following the equation proposed by McKee et al. (1983):

$$SAR = \lambda \times z \times (\ln A_0/A_z)^{-1}$$

where λ (= 0.0311 yr^{-1}) is the decay constant, z is the depth in the core (cm), A_0 is the specific activity of the excess ^{210}Pb at the surface, and A_z is the specific activity of the excess ^{210}Pb at depth z. The excess ^{210}Pb activities were determined by subtracting the average supported activity measured on samples taken from below the region of radioactive decay from the total activity. In cores # 71 and #86, the deepest sediments contained relatively young sediments (with ^{137}Cs). In these cores, the supported ^{210}Pb value was assumed to be 30 Bq kg^{-1}, which is an average of the supported activities measured in the nearby cores presented in this paper and by Unverricht et al. (2013–this issue). The ^{210}Pb-derived SAR assessment was validated using the first occurrence of ^{137}Cs as a marker of the early 1950s (Robbins and Edgington, 1975; Leslie and Hancock, 2008). The obtained activity profiles were interpreted under close consideration of the X-ray radiography and

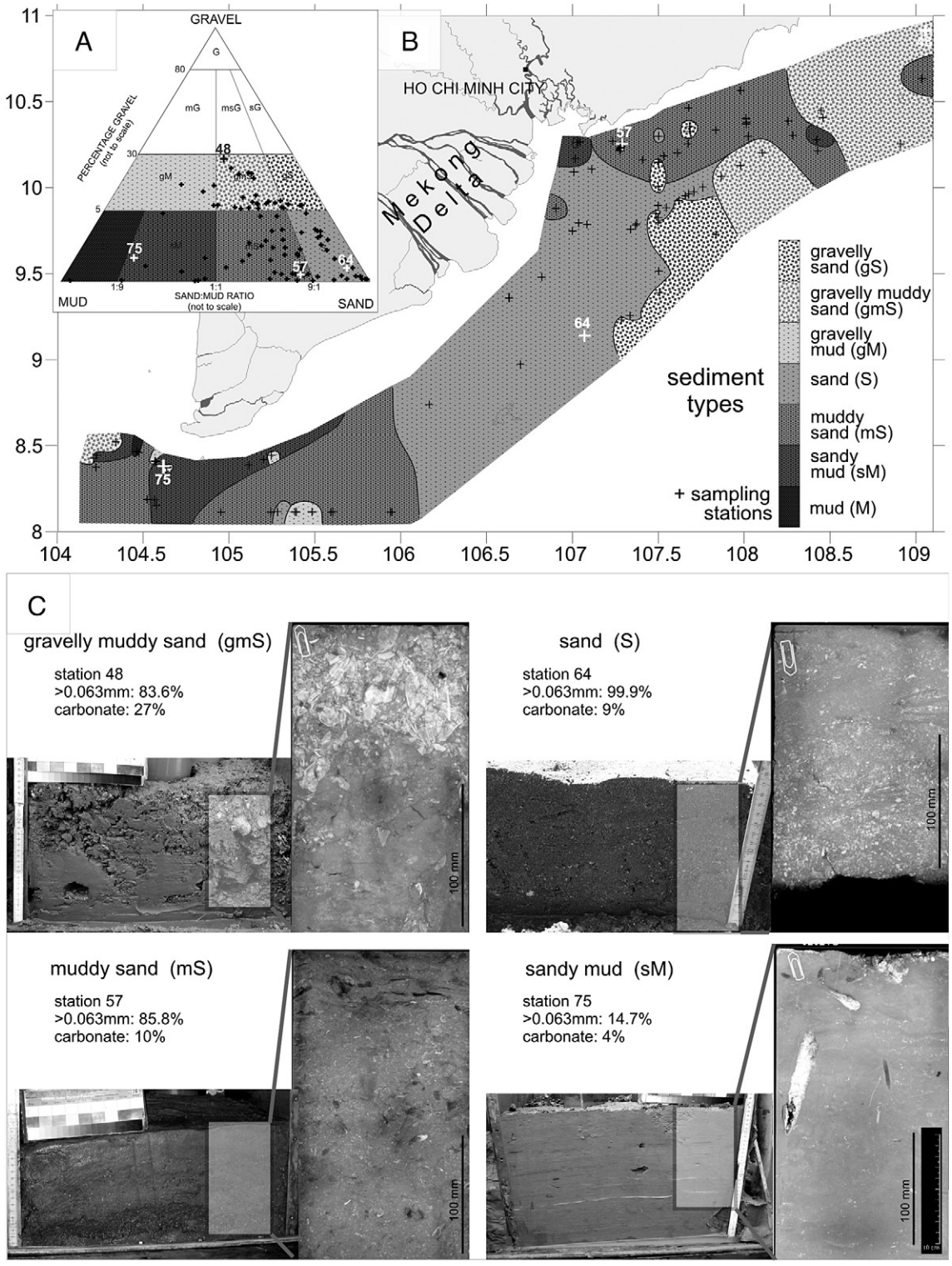

Fig. 2. Sediment textures and structures; A) All surface sediment samples placed on a gravel–sand–mud classification triangle (simplified after Folk, 1954); B) Spatial distribution of sediment types in the study area; C) Examples of box core side pictures and X-radiographs of the most common sediment types. The presented samples are marked in bold with the station number in A) and B). The values of the >0.063 mm fraction and carbonate content are given for the 0–5 cm interval.

grain-size data. However, due to relatively thick sampling intervals, evidence of non-steady sedimentation (e.g., erosional contacts) and mixing effects due to bioturbation, the calculated SARs are treated as estimates only. Further limitations of the ^{210}Pb method are discussed in Nittrouer et al. (1984), Smith (2001) and Kirchner (2011).

3.6. Statistical and GIS analyses

Basic descriptive statistics, correlation indexes and cluster analyses were performed using the Statistica 10 software. Similarities between elemental compositions were deduced from cluster analysis which

was carried out based on the Euclidean similarity using standardized data set. ArcGIS software was used to calculate areas of the regions considered in sediment budget calculations.

4. Results

4.1. Sediment types

The surface sediments in the study area are classified into seven textural groups based on the mud, sand and gravel fraction contents (Fig. 2A). The sediments are generally poorly or very poorly sorted. The major sediment types include muddy sand (31 samples), sand (25) and gravelly muddy sand (18). The subordinate deposits are sandy mud and gravelly sand present in 10 and 9 samples, respectively. Gravelly mud occurs in two samples and mud alone occurs in a single sample. The mud content of the surface sediments varies between 0.3% and 98.3% (Table 1) and is composed mostly of silt. The clay fraction (<0.002 mm) is generally less than 10% except for samples 8, 76, 77 and 81 with a clay content of up to 15% and sample 79 (mud) with a clay content of 27%.

Gravelly sand (gS) dominates in the region southeast off the Mekong River mouths where it often occurs as patches often in muddy sand or sand (Fig. 2B). This sediment type is found at stations located in water depths between 25.5 m and 44 m. The sand content ranges from 85% to 92% and the gravel fraction (primarily composed of shell hash) ranges from 5% to 10%. These sediments are very poorly sorted.

Gravelly muddy sand (gmS) covers most of the eastern portion of the study area but is also found in the westernmost and southernmost samples at water depths of 22 m to 109 m (Fig. 2B). This type of sediment is also found in spots at single sites in areas covered otherwise by sandy mud and muddy sand. This sediment is generally extremely poorly sorted with sand content of 51.6% to 75% supplemented by mud and up to 27% gravel. Shell debris (which is commonly reworked, crushed and sorted) contributes the major proportion of the gravel fraction as well as a minor amount of sand-sized material. In many cases, the gravel fraction is enriched in layers or burrow infills. The internal sediment structures are variable (Figs. 2C; 3, cores 71, 78 and 92) and include intensively bioturbated and massive beds, poorly preserved layering of extremely poorly sorted material and reworked shell debris (e.g., sample 92), and laminated silty sand intercalated with coarse shell-debris rich layers with an erosional base. However, in most cases, both the muddy sand and calcareous intervals are burrowed to a varying degree and the boundaries are churned by bioturbation (e.g., 71). The mud fraction is concentrated in burrow infills (e.g., 92) or constitutes discontinuous layers. Erosional contacts are common and are marked by truncated bioturbation burrows.

Sand (S) sediments dominate the central study area southward and southeastward off the Mekong River mouths (Fig. 2B). Moreover, this type also appears in some southernmost samples in the western portion of the area. Sand occurs in water depths ranging from 21 m to 39 m and is the only sediment type that is usually moderately sorted. The dominant grain-size fractions are fine and medium sands (Appendix 1 in the Supplementary online material). Structurally, the sands offshore of the Mekong River mouths are represented by two major types: cross-bedded, fine and medium sands, and laminated to massive well-sorted fine sands. The first type is found in samples 60 and 64 (Fig. 2C), for instance, and is characterized by a rippled sediment surface as observed from the giant box corer as well as common horizontal and cross lamination, frequent erosional contacts, minor amounts of crushed shells and a few burrows. The second type contains up to 85% of fine-grained sand and is nearly homogenous (for instance in 44, 60 and 64) or distinctly laminated (e.g., 70). The homogenous sediments are characterized by the common presence of well-preserved turritellid snails, mostly enriched on the sediment surface or close to it. In the laminated sand, certain burrows are filled with coarse sand and shells. The sand cover in the shallow area (21–27 m) next to the Mekong River distributary outlets (e.g., samples 60, 69, 61 and 70) reveals a westward trend of decreasing grain size, improved sorting and increasing abundance of burrows.

Muddy sand (mS) is the most common sediment type found at a wide range of water depths from 18 m down to 112 m. The sand contents range from 55% to 89%. Two main regions covered by this sediment type are located to the east and to the west of the central sand-covered area (Fig. 2B). The western portion of the muddy-sand area surrounds a sandy mud and mud-covered shallow shelf next to the Camau Peninsula. Muddy sand is also present over the outer shelf at the eastern edge of the study area. The sediments are extremely poorly sorted and contain commonly shell fragments. In certain cases, intact shells, mainly of snails (turritellids), appear in large abundance near the sediment surface (e.g., sample 71). The primary sedimentary structures (Figs. 2C, 3 — core 87) are overprinted by bioturbation. In certain cores, remnants of layering consisting of sand with shells interbedded with mud lenses or layers are preserved and associated with local erosional truncations (sample 67). Due to selective bioturbational mixing in several box cores the remnants of mud and sand layers form "pockets". Selected burrows are infilled with mud, although no mud layers are preserved. In several box cores, bioturbation causes the structure to appear nearly homogeneous (e.g., samples 50, 59 and 95).

Gravelly mud (gM) occurs only in two samples (76 and 77) close to the subaqueous delta front next to the Camau Peninsula at a water depth near 30 m. In principle, these deposits are composed of mud with partly preserved lamination. However, in certain burrows, sand- and gravel-sized broken shells occur, which contribute up to 15% of the total sediment mass. These burrows are usually truncated and covered by laminated mud, suggesting that non-preserved sand and gravel bed have originally existed.

The most common sediment type covering the seafloor next to the subaqueous delta around the Camau Peninsula at water depths of 26 m to 32 m is sandy mud (sM). These sediments are also present just eastward off the Mekong River mouths at 18 m to 22 m and at a single site at a 60-m water depth in the eastern portion of the study area (Fig. 2B). The sediments are characterized by relatively high water content and generally strong bioturbation but partly preserved layering or lamination. Among the bioturbation structures, burrows ascribed to ichnogenera *Helicodromites*, *Thalassinoides* and *Planolites* are common (Fig. 3 — core 86). The sand fraction is mostly restricted to individual sand layers (up to 4 cm thick), to burrows below such sand intervals, or to individual burrows (Fig. 2C), which were likely filled with sand from migrating, only temporarily present, today not preserved sand

Table 1
Descriptive statistics of the surface sediment grain size (mud content) and chemical and mineralogical (clay minerals) composition.

	Unit	Number of samples	Mean	Median	Minimum	Maximum
Mud content	%	96	20.7	14.0	0.3	98.3
Carbonates	%	96	17.2	13.0	3.0	81.0
TOC	%	92	0.2	0.2	0.0	0.9
Al	g kg^{-1}	47	43.8	35.7	5.4	97.2
Br	mg kg^{-1}	47	32.9	27.8	16.9	95.4
Ca	g kg^{-1}	47	73.7	63.1	7.8	193.9
Fe	g kg^{-1}	47	24.9	21.2	9.2	71.4
K	g kg^{-1}	47	11.6	11.2	4.8	21.1
Mg	g kg^{-1}	47	15.1	15.8	5.7	22.0
Mn	mg kg^{-1}	47	515.3	456.0	247.4	1193.1
P	mg kg^{-1}	47	434.2	446.3	134.7	768.5
S	mg kg^{-1}	47	2111.6	2028.2	858.5	7310.7
Si	g kg^{-1}	47	228.2	222.9	142.2	361.6
Sr	mg kg^{-1}	47	384.1	314.3	72.4	1044.9
Ti	g kg^{-1}	47	2.6	2.3	0.7	5.8
Chlorite	%	73	15.2	15.4	6	25
Illite	%	73	46.8	46.1	34	63
Kaolinite	%	73	18.2	19.7	2	27
Smectite	%	73	19.8	20.7	4	36

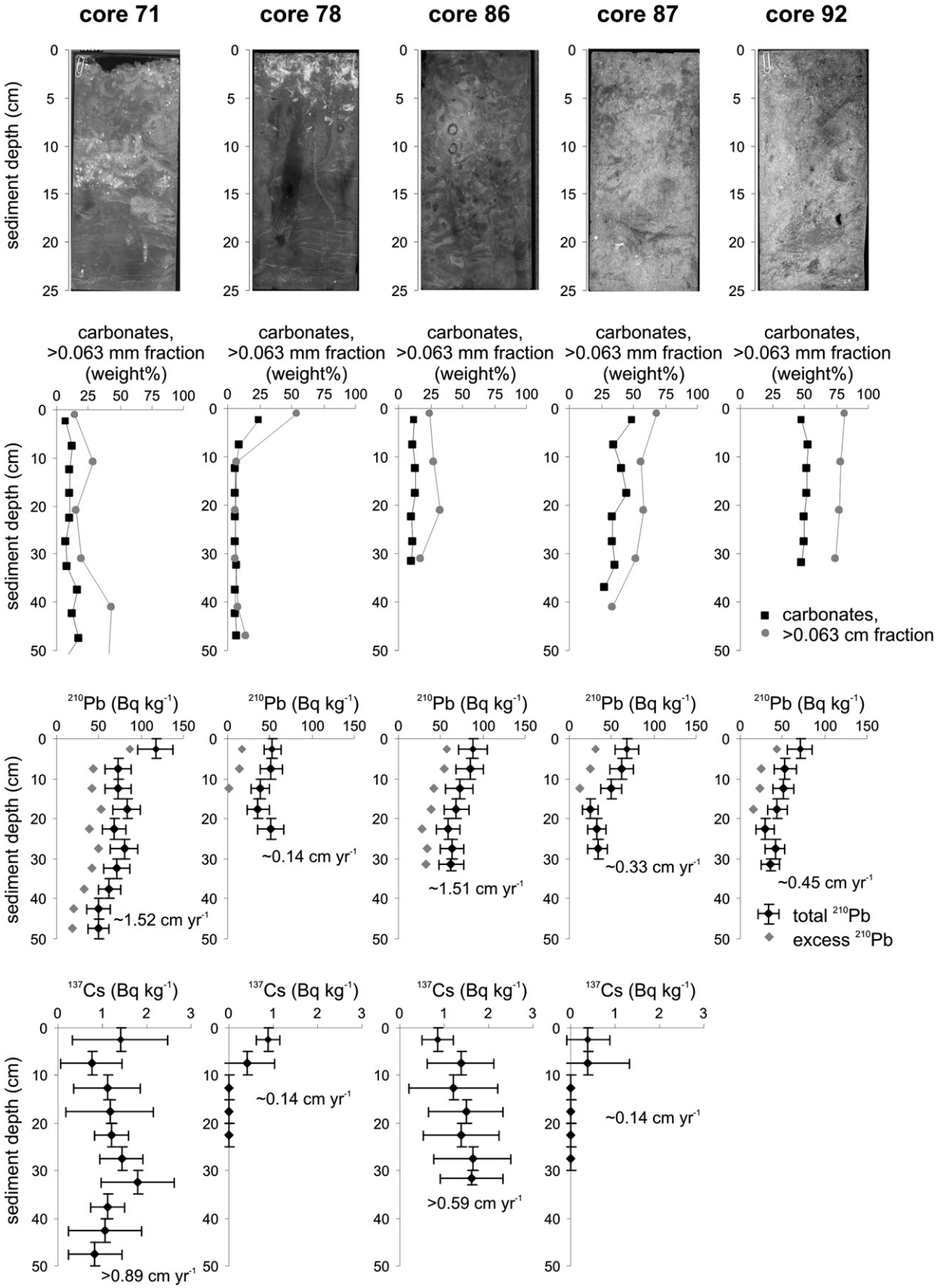

Fig. 3. Sedimentary properties (X-ray radiography, >0.063 mm fraction content, carbonate content) and ^{210}Pb and ^{137}Cs activity profiles for sediment cores 71, 78, 86, 87 and 92 taken from giant box corers. X-ray radiographs show the uppermost 25 cm of the giant box core sediments (samples taken from the side of the box corer). The vertical error bars represent sampling intervals for the samples, and the horizontal error bars indicate 2-sigma measurement uncertainties.

veneers. The sand is composed primarily of shell fragments, but large shells are generally rare.

Mud (M) sediments are found only in one sample (79), at a 30-m water depth next to the area covered by sandy mud near the western portion of the subaqueous delta front. This sediment type is similar to the sandy mud facies in the area; it is laminated and has relatively high water content. Moreover, sand layers with associated sand filled burrows are observed deeper (>5 cm) in this box core sample.

4.2. Sediment accumulation rates

The excess ^{210}Pb activity profiles (Fig. 3) reveal a generally decreasing trend with sediment depth and allow for estimation of sediment accumulation rates (SARs). However, as discussed below, due to variations in the slope of the profiles, relatively thick sampling intervals and a complex depositional history (erosion, bioturbation as revealed in X-ray radiographs), the obtained values must be treated as approximate. Nonetheless, these values are in good agreement with the SAR assessments from the maximum penetration depth of ^{137}Cs (Fig. 3).

The 52-cm-long core 71 is composed mostly of sandy mud (although the surface sample from that site is found to represent gmS). The deposit is bioturbated in the upper ~15 cm and laminated below down to at least 25 cm. Excess ^{210}Pb is present throughout the core, and the average calculated SAR is 1.52 cm yr^{-1}. However, as revealed by the profile and sedimentary structures, the sediment accumulation has varied with time. The rapid decrease in excess ^{210}Pb activity in the top samples implies a lower accumulation rate, as also suggested by the highest excess ^{210}Pb activity in the surface sample among the studied cores and the bioturbational structures present. The lower activities near a 10-cm core depth and possibly also in the lowermost region of the core may be related to the higher sand content. The majority of the core shows nearly uniform activities and together with evidence of minor bioturbated laminated sediments (Fig. 3) may reflect notably high accumulation rates (higher than the average calculated value). Additionally, ^{137}Cs is present throughout the entire core, although the measured activities are generally low (less than 2 Bq kg^{-1}) and no sharp activity peak was detected. However, the presence of ^{137}Cs throughout the core suggests that the sediments were deposited after the 1950s, and therefore the SAR is >0.89 cm yr^{-1}, which supports the estimates based on ^{210}Pb.

Core 78 is composed of gravelly muddy sand at the surface and sandy mud lower in the core. The uppermost 5 cm is rich in carbonate sand and gravel and is bioturbated, whereas the lower portion of the core is laminated with only few burrows. Excess ^{210}Pb is present only in the upper 15 cm, and the calculated SAR is 0.14 cm yr^{-1}. However, relatively low excess ^{210}Pb activity in the top sample (the lowest among the measured cores) suggests that the modern sediment surface may represent a recent erosional surface. The accumulation rate in the lower section (below 15 cm) with laminated sediments was likely higher than the calculated value. The activity of ^{137}Cs is measured only in the top 10 cm, and its activities are quite low (<1 Bq kg^{-1}). The calculated SAR of 0.14 cm yr^{-1} matches that of the ^{210}Pb measurement.

The 33-cm long core 86 is composed of initially stratified sandy mud with common bioturbation structures. Excess ^{210}Pb is present throughout the core (Fig. 3), and the average calculated SAR is 1.51 cm yr^{-1}. ^{137}Cs is also present throughout the core with low activities and suggests that the SAR is >0.59 cm yr^{-1}, supporting the ^{210}Pb-derived estimate.

Core 87 is 41 cm long and composed of sandy mud and muddy sand. This core contains remnants of stratification but is dominated by bioturbational structures (Fig. 3). The SAR assessed from ^{210}Pb profile is approximately 0.33 cm yr^{-1}. The ^{137}Cs penetration depth is 10 cm, indicating an SAR of approximately 0.14 cm yr^{-1}, which is less than that calculated from ^{210}Pb. However, the ^{137}Cs activities are notably low (<0.5 Bq kg^{-1}), possibly partially due to the high carbonate-sand content (33–68%), which could also cause dilution of the radioisotope in the deeper samples. Thus, the estimated ^{137}Cs-derived SAR should be treated as a minimum value.

Core 92 is composed of bioturbated gravelly muddy sand with certain remnants of layering. Excess ^{210}Pb decreases with depth (Fig. 3), and the calculated SAR is 0.45 cm yr^{-1}. The ^{137}Cs value is below the minimum detection activity and is likely due to the high carbonate-sand content (74–82%).

4.3. Clay mineral distributions

The spatial distribution of clay minerals reveals substantial variations despite the nearby single major sediment source, i.e., the Mekong River (Fig. 3, Table 1, Appendix 1 in the Supplementary online material). The most common mineral is illite; its average content is 46% and its contribution is in the range of 33% to 63% of all clay minerals. Illite is the most common mineral in the area located in a straight line off of the major Mekong River branches and west of the Camau Peninsula. The lowest values appear along the coast eastward from the Mekong River delta. Chlorite is the least common mineral, with an average of 15%. The spatial variability of its contribution is similar to that of illite, except in an area in the northeastern portion of the study area where a relatively higher amount of chlorite is associated with the lowest amount of illite. Smectites and kaolinite exhibit similar average contents of 19% and 18%, respectively, but their spatial variability is quite different. The contribution of smectites generally increases with distance from the Mekong River mouths and its variability anti-correlates with that of illite in principle. In contrast, the contribution of kaolinite is relatively uniform except for a region eastward of the Mekong River delta where sediments with a kaolinite content greater than 20% form a belt parallel to the coastline.

4.4. Sediment geochemistry

The spatial variability of geochemical data is presented in a series of figures (Figs. 5–7), and the descriptive statistics are listed in Table 1. Table 2 presents a correlation matrix of the elements, and the complete data set is presented in Appendix 1 of the Supplementary online material.

4.4.1. Carbonate content

The carbonate content in the sediments varies over a wide range (Table 1, Fig. 5). In general, the sediments collected close to the Mekong River mouths are the poorest in carbonate (as low as 3–4%), and a clear offshore-increasing trend is observed. In samples from further on the shelf, the carbonate content reaches 20–40%, with a maximum value of 81% (sample 89). The carbonate content correlates well with the Ca concentration (Table 2).

4.4.2. TOC

The lowest TOC contents of 0.02–0.05% are found in samples at water depths from 20 m to 35 m collected to the southeast and south of the Mekong River mouths (Fig. 3). The TOC content increases toward the west, southwest and toward the coast, reaching maximum values of 0.7–0.94% in samples collected close to the subaqueous delta front around the Camau Peninsula and directly next to the Mekong River mouths. The TOC also increases in an eastward direction from the area of its minimum content. However, the maximum values in that region are lower (0.33–0.42%) and are found in samples from relatively deep waters (47 to 60 m); there is no single trend in variability. The distribution of TOC correlates well with the mud content (Table 2).

4.4.3. Bulk elemental composition

Among the analyzed elements, the highest average concentrations on the order of tens to hundreds of g kg^{-1} are of Si, Ca, Al, Fe, Mg and K (Table 1). The minor components in decreasing order are Ti, S, Mn, P, Sr and Br. The spatial variability in the concentrations is similar for several of these elements, namely for Al, K and Ti or for Ca and Sr,

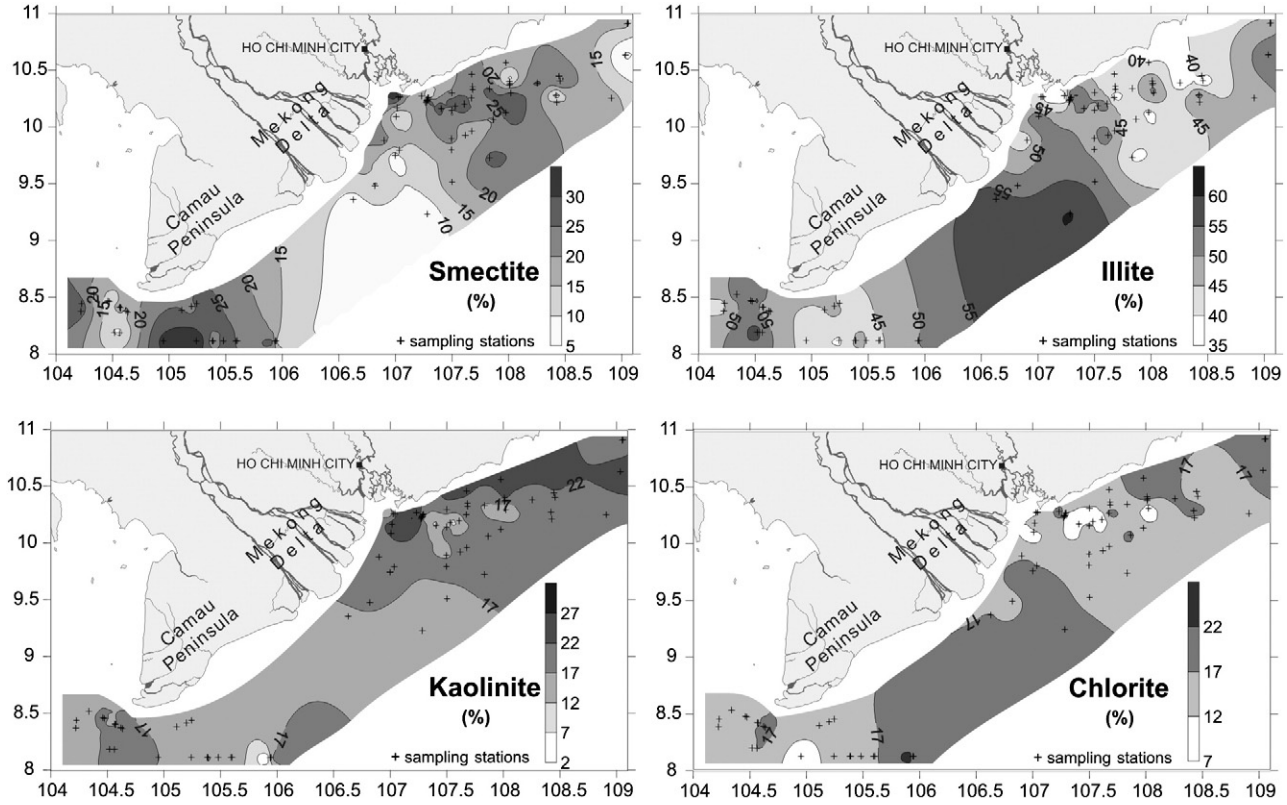

Fig. 4. Distribution of smectite, illite, kaolinite and chlorite in the <0.002 mm fraction in the study area. Relative clay mineral abundances are given as a percent of their sum. The interpolation is performed using a kriging method.

suggesting the common presence in phyllosilicates and calcium carbonate minerals, respectively.

The Si concentration is the highest in the sand-dominated sediments (with mud content of less than 1%) located south and southeast of the Mekong River mouths (Fig. 6). However, the Si concentration is also moderately high in the mud-dominated areas around the Camau Peninsula. The lowest Si concentration occurs in the southernmost and in eastern parts of the study area. The Si distribution is negatively correlated with the carbonate-related elements Ca, Sr and Mg as well as with carbonate content (Table 2).

The spatial variations in the concentrations are almost identical for Ca and Sr (correlation coefficient 0.97). Their concentrations span three orders of magnitudes and are the most variable components of the studied elements. The spatial distribution is the opposite of that of Si, with the highest Ca concentrations found in gravelly muddy sands in the southernmost and eastern parts of the study area. The lowest values are found close to the Mekong River mouths and around the Camau Peninsula, and a general offshore-increasing trend is observed in the concentrations of Ca and Sr.

The concentration of Al, K and Ti co-varies (Fig. 6, Table 2). The maximum values are found around the Camau Peninsula, in muddy sediments just eastward of the Mekong River mouths and in moderately high concentrations in the northeastern portion of the study area. The concentration variability of Al, K and Ti correlates well with the mud and TOC contents (Table 2). To a certain extent, similar spatial distribution patterns are observed for S, Mn, Fe and Br.

The spatial variability of Fe closely resembles those of Al, K and Ti, except for the sand-dominated area southeast of the Mekong River mouths, where the Fe content is relatively high. Apart from the mentioned elements, Fe is also well correlated with Mn.

The area located just eastward of the Mekong River mouths shows the highest Mg concentrations. However, this element is also abundant

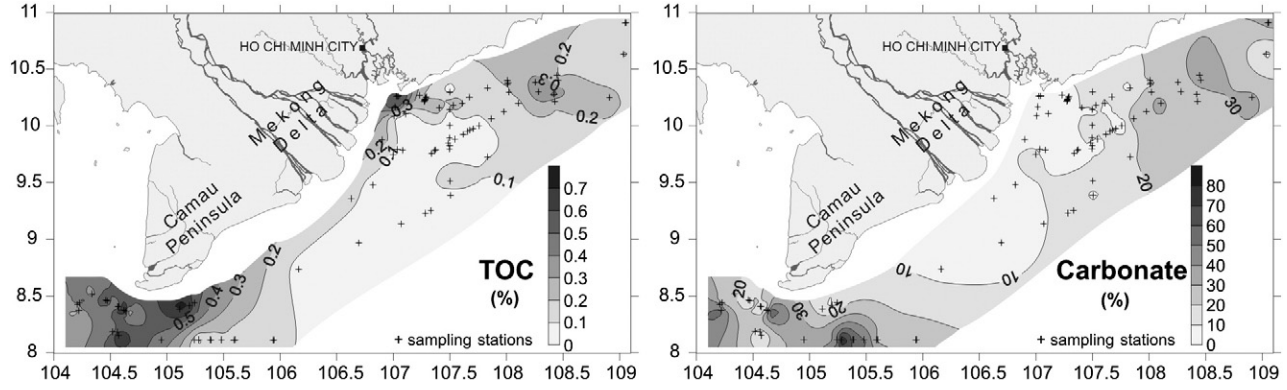

Fig. 5. Distribution of TOC (%) and carbonates (%) in the surface sediments of the study area. The interpolation is performed using a kriging method.

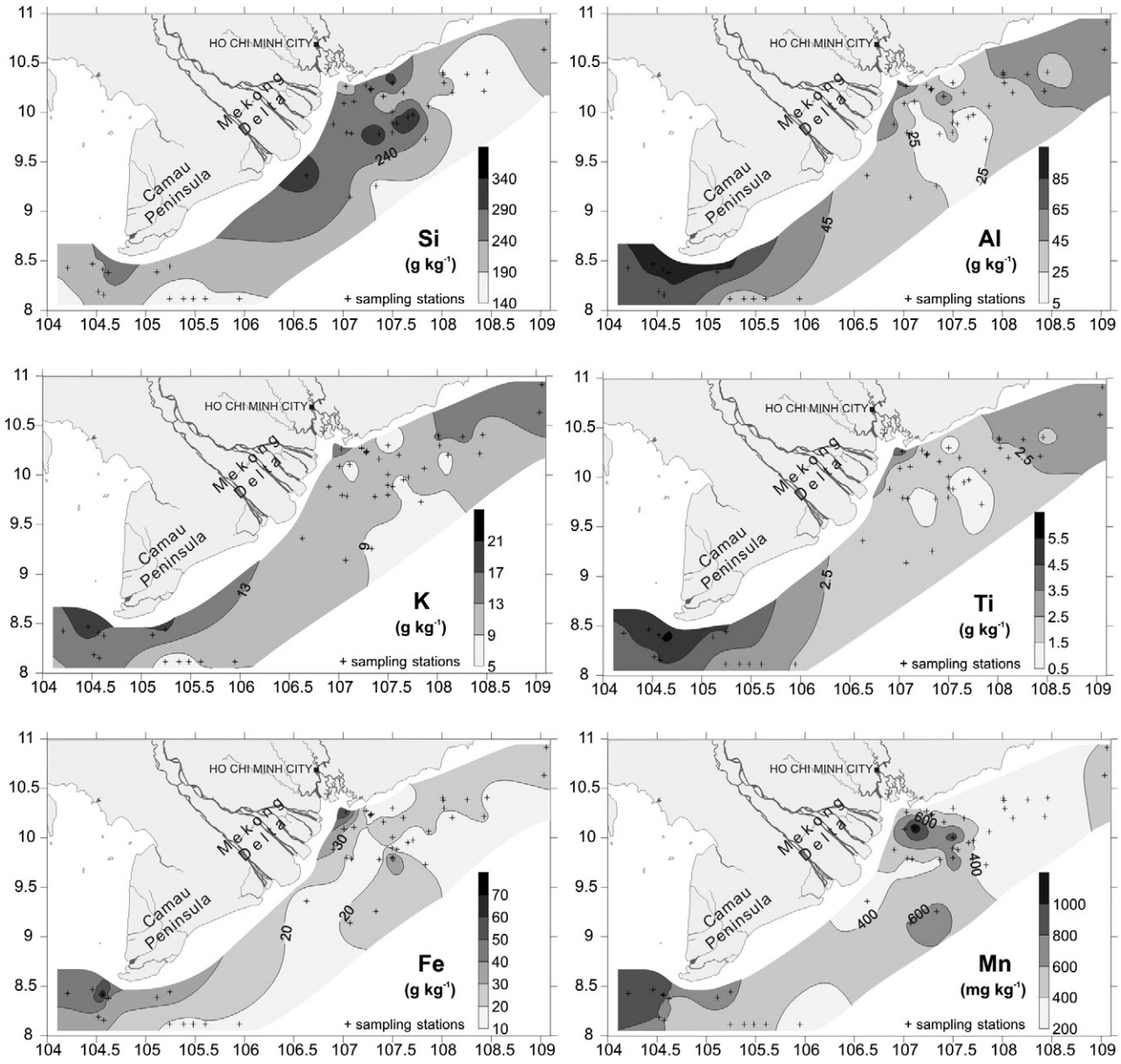

Fig. 6. Distribution of total contents of elements Si, Al, K, Ti, Fe and Mn in the surface sediments of the study area. The interpolation is performed using a kriging method.

in sediments westward and eastward of the Camau Peninsula and in the southwestern study area. The minimum values are found near the maximum values, on the shelf southeast of the Mekong River mouth and next to the Camau Peninsula. In general, the spatial distribution of Mg is similar to that of the carbonate content and the Ca and Sr concentrations.

The S content is highest next to the subaqueous delta front around the Camau Peninsula, where an outstanding value of 7310.7 mg kg^{-1} was observed in sample 75 (double the second highest concentration). Sulfur also shows a high concentration just eastward of the Mekong River mouth, but its content is much lower further offshore. This element correlates well with the TOC content.

The spatial distribution of Mn is characterized by maximum values in sands located southeast of the Mekong River mouths and in muddy sediments westward of the Camau Peninsula. The lowest concentrations are measured not only in the eastern portion of the studied area but also in sands just south of the Mekong River mouths. Although the variability of Mn concentration seems to be irregular, the correlation analysis reveals a similarity to Fe and Br, and partially follows the changes in mud, TOC, Al, K and Ti content.

The P concentrations are highest in the most distal samples southeast of the Mekong River mouths and westward of the Camau Peninsula. The lowest concentrations are found eastward of the Mekong River mouths. This spatial pattern is quite different from that of the other elements and the highest correlation coefficient value is 0.51, suggesting a vague correlation of P with Fe.

The area surrounding the Camau Peninsula shows the highest concentration of Br. The second area with a slightly elevated concentration is located in the eastern portion of the study area. The spatial variability of Br correlates well with the mud content and with the Al and Ti concentrations.

5. Discussion

5.1. Dispersal pattern of Mekong River-derived sediments on the continental shelf

Tide-influenced deltas such as the Mekong River delta are commonly divided into a subaerial region (delta plain) and a subaqueous region. The latter is composed of a delta front (delta front platform and slope)

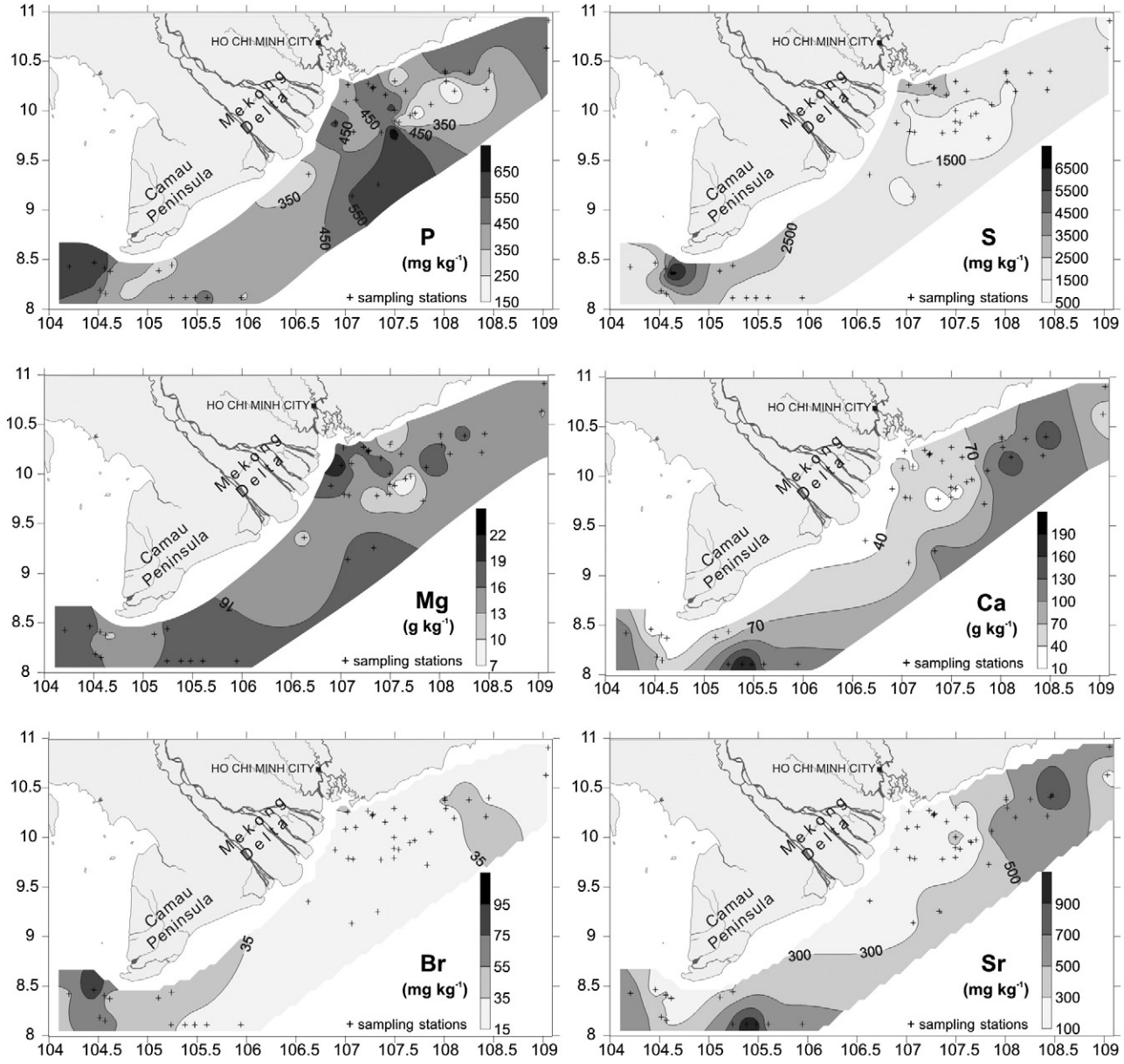

Fig. 7. Distribution of total contents of elements P, S, Mg, Ca, Br and Sr in the surface sediments of the study area. The interpolation is performed using a kriging method.

Table 2
Correlation coefficient matrix of the analyzed elements and compounds. Bold indices are significant at the $p < 0.05$ level of confidence.

	Mud	$CaCO_3$	TOC	Mg	Al	Si	P	S	Cl	K	Ca	Ti	Mn	Fe	Br	Sr
Depth	−0.24	0.01	−0.26	−0.27	0.00	−0.10	0.24	−0.30	−0.28	0.14	0.02	−0.08	−0.24	−0.13	−0.29	0.06
Mud		−0.26	**0.87**	−0.02	**0.84**	0.16	0.33	**0.62**	0.11	**0.65**	−0.41	**0.93**	**0.67**	**0.67**	**0.86**	−0.27
$CaCO_3$			−0.35	**0.69**	−0.43	**−0.80**	−0.20	−0.26	−0.03	**−0.67**	**0.96**	−0.21	−0.16	−0.31	−0.26	**0.99**
TOC				−0.21	**0.86**	0.28	0.03	**0.76**	−0.08	**0.65**	−0.51	**0.88**	**0.55**	**0.60**	**0.67**	−0.38
Mg					−0.13	**−0.71**	0.13	−0.24	0.24	−0.30	**0.67**	0.01	0.12	−0.01	0.15	**0.70**
Al						0.22	0.38	**0.56**	−0.01	**0.88**	−0.57	**0.93**	**0.67**	**0.83**	**0.77**	−0.42
Si							−0.03	0.19	−0.29	0.44	**−0.86**	0.10	0.19	0.18	0.03	**−0.83**
P								−0.02	0.08	0.47	−0.23	0.35	0.44	**0.51**	0.39	−0.18
S									−0.14	0.29	−0.35	**0.66**	0.25	0.44	0.30	−0.29
Cl										−0.06	0.08	−0.01	0.17	0.07	**0.45**	−0.01
K											**−0.75**	**0.70**	**0.55**	**0.72**	**0.68**	**−0.64**
Ca												−0.38	−0.32	−0.44	−0.33	**0.97**
Ti													**0.70**	**0.77**	**0.77**	−0.21
Mn														**0.81**	**0.70**	−0.17
Fe															**0.68**	−0.29
Br																−0.24

attached to the coast and a prodelta located further offshore (e.g., Goodbred and Saito, 2012). Recent advances in studies on the Mekong River delta system revealed that the subaqueous delta front progrades in two directions, directly offshore of the river mouths and in the western direction around the Camau Peninsula (Fig. 1). It was found that the delta front is up to 20 km wide and is bound offshore by a rapid change in slope inclination. This rapid transition is also documented by a change in the prevailing sediment type, from well-sorted sands or poorly sorted silts on the delta front to medium and coarse sands with shell fragments further offshore of the delta front slope (Anikiev et al., 2004; Xue et al., 2010; Unverricht et al., 2013–this issue). However, a modern prodelta was not yet identified.

Prodeltas of large tide-influenced rivers, as reviewed by Hori and Saito (2007) and Goodbred and Saito (2012), are typically 20–50 km wide and are often composed of bioturbated muds intercalated with shell beds. The previous study by Anikiev et al. (2004), which focused on an area south of the Mekong River mouths (Fig. 1), showed that mud deposits are located only in a narrow belt next to the coast in a water depth near 10 m. However, most of the shelf adjacent to the delta is covered by sands of various compositions, and certain of them are interpreted as relict deposits. The eastern portion of the shelf was partly studied by Kubicki (2008) who found frequent fields of sand dunes instead of typical prodelta sediments. In contrast to these previous studies, the current study clearly reveals a large area of mud-dominated sediments (M, gM and sM) located in the west of the delta mouths around the subaqueous delta front next to the Camau Peninsula (Fig. 2). These deposits are characterized by high SARs (0.1–1.5 cm yr^{-1}), common bioturbation structures and the presence of intercalated shell beds. This mud-rich area extends for at least ~30 km in the southwest and west and most likely represents the subaqueous prodelta of the Mekong River delta.

Moreover, a high proportion of mud was also found in those shelf sediments (mS and gmS), which cover wide areas of the shelf in the southernmost offshore region as well as in the northeast (Fig. 2). To determine if these materials are derived from the modern Mekong River, their clay mineralogy and bulk geochemistry were studied. Clay mineral assemblages in marine sediments are often used as a tracer with respect to their source and the weathering conditions on the surrounding continents (e.g., Gingele et al., 2001; Liu et al., 2003; Steinke et al., 2008). However, the applications of clay minerals involve several limitations of which the major one is that most of the reported results are of a semi-quantitative nature and are largely affected by differences in preparation procedures and the interpretative approach of the resulting X-ray diffractograms (Thiry, 2000). Because of these issues, it is often difficult to compare quantitative results from different studies, and only relative trends should be considered.

Illite is the dominant clay mineral in the current study as well as in the previous studies from the Mekong River delta and from the southwestern South China Sea shelf region (Aoki, 1976; Chen, 1978; Jagodziński, 2005; Liu et al., 2007; Xue et al., in press). Illite is considered as a primary mineral that reflects the increased rock weathering under cold and arid climatic conditions. In the studied case, illite could be derived from physical erosion of metamorphic and granitic rocks mostly located at high elevation in eastern Tibet (Liu et al., 2007).

The presented spatial distribution of clay minerals (Fig. 4) shows a major trend with the increasing distance from the Mekong River mouths reflected by a decrease in illite and chlorite on account of smectite. A similar trend of westward increasing content of smectite was reported by Xue et al. (in press) in short sediment cores taken from the subaqueous delta sediments. According to this group, this trend implies a reduced fine sediment input from the Mekong River on account of certain other unspecified sediment source. However, considering the large volume of fine-grained sediments accumulating at rates of at least several cm per year, it is unlikely that the sediments from other unknown sources would contribute significantly in the areas of the highest accumulation rate. The trend of an increasing content of smectite in the offshore direction is documented on several continental shelves adjacent to large rivers, i.e., the Niger (Porrenga, 1966, 1967) and Amazon (Patchineelam and de Figueiredo, 2000), and is also described for continental margin settings (Thiry, 2000). These trends were explained by differential settling of smectite versus other clay minerals. Although the processes and governing factors behind this observation are still under discussion (Thiry, 2000), smectites are generally believed to flocculate preferentially in more saline waters, and thus they settle down farther offshore than other clay minerals. It is likely that the same process applies for the current case as well.

The northeastern portion of the studied area is characterized by the highest contents of kaolinite and chlorite and the lowest contents of illite, whereas the illite and chlorite contents correlate well with each other in most other portions of the studied shelf (Fig. 4). These relative changes suggest that clay size fraction sediments in the northern portion of the shelf may be at least partly contributed from another source, i.e., from the small mountainous rivers entering the sea just to the east and northeast of the Mekong River delta (e.g., Saigon River). The total contribution from these minor but numerous river sources is likely relatively small because the clay fraction in these sediments sums to only a few percent. In addition, shallow seismic studies indicated that no major modern sediment accumulation body is present in this area (Kubicki, 2008; Tjallingii et al., 2010).

The bulk geochemistry analysis reveals distinct spatial variations of the particular elements, which were found to correlate primarily with such major sediment properties as grain size and carbonate content. To reveal the spatial variations between the geochemical compositions of particular samples, a statistical cluster analysis was performed (Fig. 8) and the results show three distinct groups of samples that refer to geographically separated regions in Zones referred to as A to C (Fig. 9; Table 3).

Zone A covers the shallowest portion of the study area with water depths no deeper than 32 m. This zone is primarily composed of samples from sites around the Camau Peninsula and next to the Mekong River mouths. The dominant sediment types are sandy mud and gravelly muddy sand (M, gM, mS, S, sM and gmS). The SARs are relatively high, reaching up to 1.5 cm yr^{-1}. The major properties of sediments from Zone A are a high mud content (over 50%, on average) and the highest content of TOC. Moreover, these sediments are characterized by the highest concentrations of Al, Ti, Fe, S and Br. The content of carbonates is higher than in Zone B but much lower than in Zone C.

Zone B represents transitional settings in terms of water depth (32 m on average) compared with the other two zones and is dominated by sandy deposits (S, mS and gS) with an average sand content greater than 90% and a low carbonate content. The highest concentrations of Si are noted in this zone as well as the lowest contents of carbonate, TOC, Al, Ti, Sr and Br.

The samples located the furthest offshore are those from a group in Zone C characterized by poorly sorted muddy sands (mS and gmS). These deposits are rich in carbonate shells and the highest contents of carbonate, Ca and Sr are accompanied by the lowest contents in Si and P. The samples from the western portion of this zone show the highest contents of carbonate, whereas those from the eastern portion are characterized by higher Si and Fe contents.

The mud-dominated, organic-rich, high-accumulation Zone A represents the Mekong River prodelta. Zone B, located southward from the river mouths and dominated by terrigenous sands, covers the area in which bedload-transported material from the Mekong River is highly important. The most distantly located offshore Zone C is dominated by muddy sand with a strong contribution of biogenic carbonates. Because the clay mineral contents are similar in all zones, it is likely that Zone C receives a minor contribution of fine-grained sediments, possibly from the Mekong River in its western part. In the eastern section, the finest sediments may originate from the Mekong and in the northeastern part as well as from selected other sources.

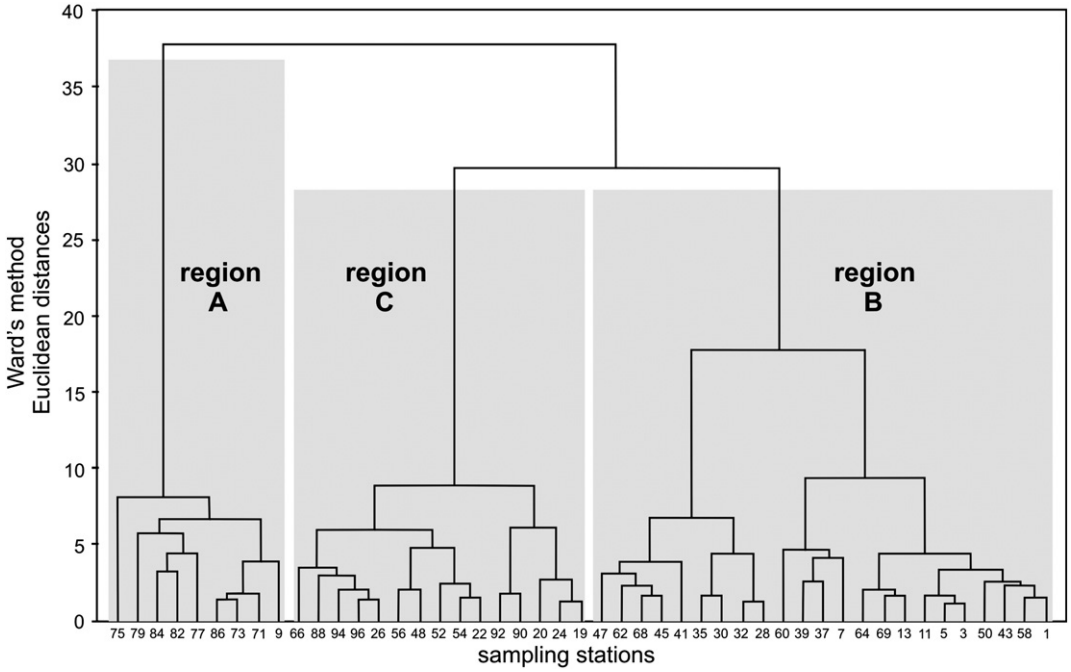

Fig. 8. Results of cluster analyses of surface sediments based on their chemical compositions. A small Ward's distance indicates that the assemblages are similar. Regions A, B and C refer to the sample clusters discussed in the text.

5.2. Modern sedimentary processes

The presented data on sedimentary properties and accumulation rates also provide insight into the depositional processes that dominate in the muddy prodelta (Zone A), on the inner shelf covered by terrigenous sands (Zone B), and offshore shelf zone dominated by muddy carbonate sands (Zone C).

5.2.1. The prodelta (Zone A)

The mud-dominated sediments (M, gM and sM) of the prodelta located southwest from the Camau Peninsula (Fig. 9) are characterized by high accumulation rates of a few mm to ~1.5 cm per year. These rates fall within the range of values reported for prodeltas of other large rivers such as the Ganges–Brahmaputra, Changjiang or Amazon (e.g., McKee et al., 1983; Kuehl et al., 1985; Michels et al., 1998). In addition, erosional contacts are common in the succession of these deposits, which suggest that the short-term (e.g., seasonal) deposition rate often may be much higher than the ^{210}Pb-derived 100-year timescale averages reported, e.g., for the Changjiang prodelta by McKee et al. (1983).

The changing depositional conditions are reflected in the sediment types and structures. The prodelta deposits consist of laminated mud, bioturbated mud, and carbonate-dominated sand and gravel intercalations and/or burrow infills. The laminated deposits and coarse-grained sediments were likely formed during rapid depositional events, whereas in general the bioturbated mud-dominated sediments reflect periods of lower accumulation rate (see Section 4.2).

The rapid depositional events are most likely related to redeposition from the subaqueous delta front, which is strongly affected by waves and tides. Unverricht et al. (in press) reported that even during intermonsoon seasons and neap-tide conditions when the tidal currents, wind waves and wind-generated currents are weakest, resuspension of the delta front sediments is common. During spring-tide conditions and a fully developed monsoonal wind and current regime, the resuspension is expected to be much more intense. Several possible modes of sediment redeposition exist, including winnowing due to high waves during typhoons, tidal currents or seaward flow of fluid mud at the sediment/water interface (e.g., Wright and Friedrichs, 2006; Nittrouer et al., 2007). The presence of mud and sand/gravel layers suggests event transport under conditions of suspended sediment-rich or suspended sediment-poor conditions and in various transport directions. The mud is likely transported primarily in the offshore direction from the subaqueous delta front, whereas the carbonate-rich coarse-grained sediments result from an onshore-directed transport from the outer shelf (Zone C), e.g., during tropical storms.

In certain cases, the only evidence of temporary emplaced coarse-grained layers is the preserved sediment infill in burrows; their presence suggests that the prodelta area is occasionally affected by conditions leading to the erosion of coarse-grained sediments.

5.2.2. The sandy inner shelf (Zone B)

The inner shelf located eastward of the muddy subaqueous prodelta and offshore of the subaqueous delta front is dominated by moderately sorted sands just south of the Mekong River mouths and poorly sorted muddy sands with an amount of carbonate sand and gravel admixtures in the eastern part of the study area. SAR assessments for these areas are not available. However, the moderately sorted sands are likely supplied via Mekong River bedload transport, and therefore, the SARs must be relatively high because they contain hardly any in-situ produced carbonate shells, which would be expected in the case of lower accumulation rates. The relatively good sorting may result from either the supply of already well-sorted fluvial sands or from an active sorting process on the inner shelf. The latter is evident from the rippled sediment surface, internal cross-bedding and notably few burrows, implying repeated reworking. In contrast, the poorly sorted muddy sands are richer in shell debris and the primary internal structures are often overprinted by burrows. These characteristics point to relatively low accumulation rates. Because these sediments are similar to those on the outer shelf (Zone C), where the obtained accumulation rates are up to 0.4 cm yr^{-1}, one may speculate that average rates of a few mm per year might be possible in this region.

The notably small contribution of mud fraction on the inner shelf in front of the Mekong River mouths and further southward where relict deposits were found (Anikiev et al., 2004) suggests that the suspended

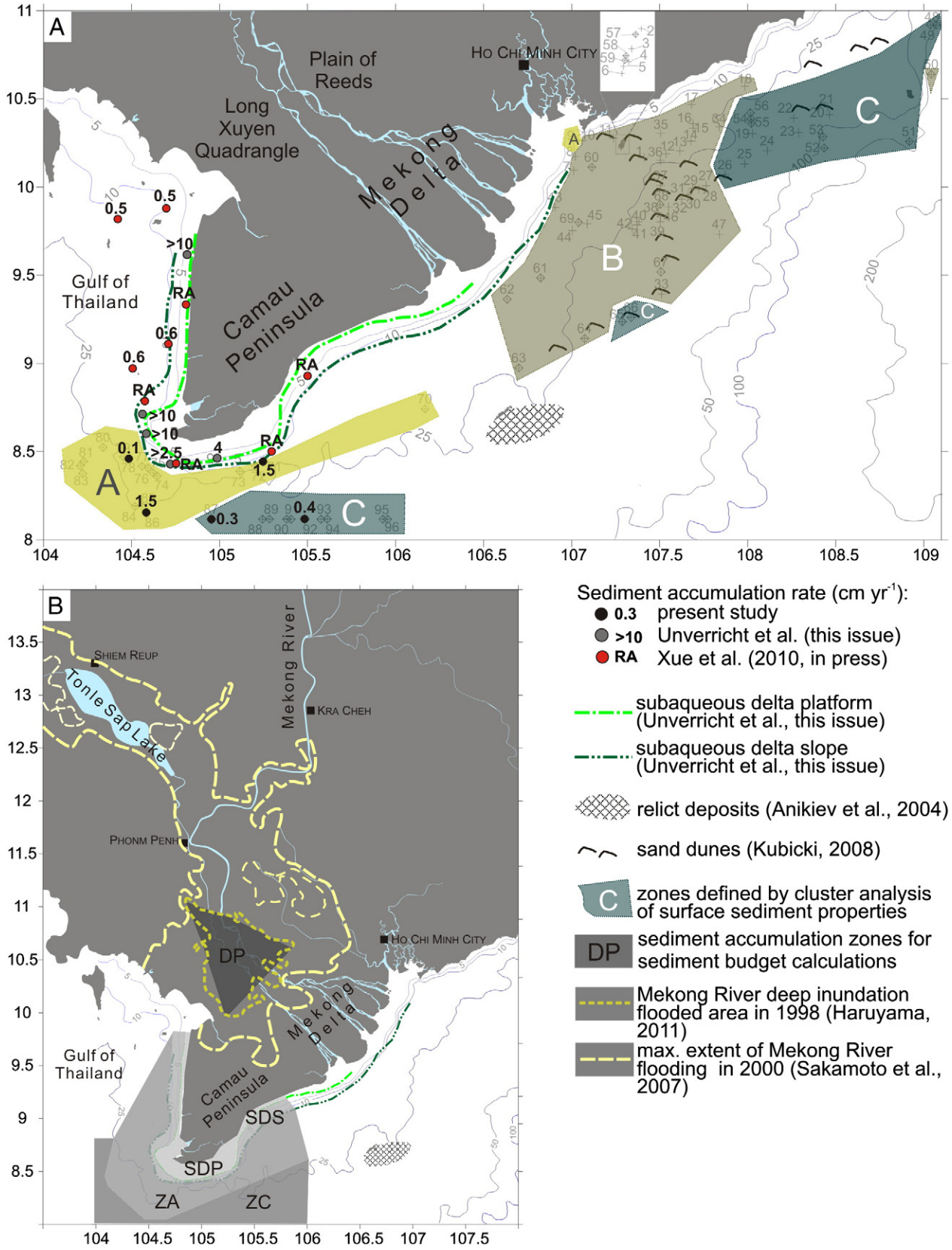

Fig. 9. Compilation of the obtained results on the sediment dispersal pattern offshore of the Mekong Delta and SARs and areas used for estimation of the Mekong River-derived fine-grained sediment budget; A) Sedimentary zones (A, B and C) obtained with cluster analysis (Fig. 8) and marked on the study area (see Fig. 1 for explanations). SARs are compiled from ^{210}Pb and ^{137}Cs dating on the subaqueous delta (Xue et al., 2010, in press; Unverricht et al., 2013–this issue) and from offshore areas (current study). RA — indicates "rapid accumulation" or "non-steady accumulation" (with excess ^{210}Pb present throughout the sediment cores) in works by Xue et al. (2010, in press). Areas covered with subaqueous sand dunes (Kubicki, 2008) and relict deposits (Anikiev et al., 2004) are marked for comparison; B) Areas selected for the fine-grained Mekong-derived sediment budget: DP — delta plain, SDP — mud-dominated portion of the subaqueous delta platform (after Unverricht et al., 2013–this issue), SDS — mud-dominated portion of the subaqueous delta slope (after Unverricht et al., 2013–this issue), ZA — mud rich parts of zone A (prodelta) and ZC — zone C. The maximum extent of river flooded area is based on major floods in 1998 and 2000 as reported by Haruyama (2011) and Sakamoto et al. (2007).

Table 3
Comparison of characteristics and surface sediment compositions in the Zones A, B and C as defined by the cluster analysis (Figs. 8 and 9). Numerical values are presented as means, and minimum and maximum values are provided in brackets. Sediment types: gmS — gravelly muddy sand, sM — sandy Mud, S — sand, mS — muddy sand.

	Unit	Zone A	Zone B	Zone C
Water depth	m	28.1 (23–32)	32.3 (18–109)	44.4 (32–112)
Sediment accumulation rates	cm yr^{-1}	0.1–1.5	Low	0–0.4
Dominating sediment types	–	gmS, sM	S, mS	mS, gmS
>0.063 mm fraction	%	46.2 (1.7–95.8)	91.1 (40.1–99.7)	79.4 (41.6–98.4)
Smectite	%	19.3 (5–36)	19.6 (6–33)	20 (4–34)
Illite	%	48.8 (42–63)	46.8 (36–60)	46 (34–60)
Carbonates	%	18.9 (3–64)	10.6 (3–36)	28.9 (4–81)
TOC	%	0.5 (0.06–0.94)	0.14 (0.02–0.71)	0.2 (0.06–0.46)
Al	g kg^{-1}	82.6 (68–97)	30.1 (5–62)	41 (25–58)
Si	g kg^{-1}	223.1 (195–265)	259.3 (173–362)	178 (173–223)
Ti	g kg^{-1}	4.6 (4–5.7)	1.8 (0.7–3.4)	2.5 (1.6–3.2)
Fe	g kg^{-1}	43.5 (33–71)	20.4 (9–47)	20.7 (15–31)
Ca	g kg^{-1}	49.2 (8–119)	53.6 (14–108)	122.8 (46–194)
P	mg kg^{-1}	466 (337–620)	446 (134–768)	406 (186–595)
S	mg kg^{-1}	3298 (2138–7310)	1757 (858–3283)	1961 (1484–2422)
Br	mg kg^{-1}	56.4 (36–95)	23.8 (17–35)	33 (27–47)
Sr	mg kg^{-1}	318.6 (115–677)	259.8 (72–634)	630.4 (505–1044)

load must be effectively transported mainly in the southwest direction toward the prodelta. An additional westward transport of sands is evidenced from a grain-size fining trend in the sediments and from improved sand sorting in this direction in the shallow area next to the Mekong River mouths. Moreover, in the eastern portion of the sand covered area Kubicki (2008) documented frequent presence of asymmetrical sand dunes. Their orientation corresponds to the direction of the westward current induced by the regional winter-monsoon winds (to SW and S). The large size of the dunes (length up to >600 m and height up to >10 m) together with theoretical calculations suggest that the near-bottom current velocity must be at least 1 m s^{-1} during the winter-monsoon season (Kubicki, 2008).

During the summer monsoon, when winds are directed toward the NE, certain fine-grained Mekong-derived sediments are likely deposited in the area composed of muddy sand. The clay mineral composition of most of the samples is similar to that of muds deposited in the prodelta next to the Camau Peninsula. However, the mud is usually only preserved in lenses and seldom as layers, and often, the only record of temporary mud deposition is preserved in the form of muddy infill of burrows. These remnants of mud deposition show that a suspended-sediment transport toward the east (documented also by in-situ measurements (Anikiev et al., 1986)) leads to temporary mud deposition. However, this mud may become remobilized and transported in the westward direction during the next winter monsoon season by the same currents, which generates the subaqueous sand-dune migration.

In sand-dominated areas, intact snail shells (turritellids) appear in large abundance on or just beneath the sediment surface. Their presence represents the only in-situ shell remnants that are locally common and are not significantly reworked. Mud deposition is often low to absent at those sites with high turritellids abundance. These turritellids are known to occur in areas in which primary production is enhanced by river-dissolved loads.

5.2.3. The muddy carbonate sands on the outer shelf (Zone C)

The outer shelf sediments are dominated by a coarse-grained carbonate fraction. The SARs in the western portion of the study area are on the order of 0.3–0.4 cm yr^{-1}. The clay-mineral composition suggests that the fine-grained fraction originates from the Mekong River. The coarse-grained fraction is composed mainly of reworked shells. Their presence suggests that bedload transport is sufficiently strong in this area to cause reworking of this material, which is in accordance with the formation of subaqueous sand dunes in the eastern portion of the outer shelf (Kubicki, 2008). The sediments are bioturbated, and primary structures are not preserved except for occasional erosional contacts, which likely formed during tropical storm events, which pass this region at least once every few years (UNISYS, 2013).

5.3. Modern sediment budget of fine-grained sediments delivered by the Mekong River

The present study of the adjacent shelf sedimentary system in concert with a number of recent studies quantifying sediment accumulation in various parts of the system (i.e., Tonle Sap Lake, Mekong Delta Plain, subaqueous delta; Kummu et al., 2008; Xue et al., 2010, in press; Hung et al., in press-a; Unverricht et al., 2013–this issue) allows for calculating a first-order modern (past 100 years) sediment budget for the fine-grained sediments supplied by the Mekong River (Table 4). Rivers transport sediments as suspended load and bedload. Commonly, the suspended load is measured with some accuracy, while the estimate of the bedload transport is difficult and virtually unknown for the large rivers (Milliman and Syvitski, 1992). Thus, although the bedload transport of coarser material to the ocean must be assumed to play an important role, the present calculation focuses on the fine-grained material (mud) only, which dominates suspended load in the Mekong. According to Wolanski et al. (1996), the suspended sediments are composed of clayey silt (mean 2.5 to 3.9 μm) in the lower Mekong distributaries. It is in agreement with data from Phnom Penh — some 340 km upstream from the river mouth (Gagliano and McIntire, 1968) and with grain size (median 10 to 15 μm) of sediments collected in sediment traps during Mekong River floods (Hung et al., in press-a).

Data on the suspended sediment discharge of the Mekong River are not available for the river mouth region and thus, the existing assessments are mainly based on the data from Pakse (~800 km upstream). Milliman and Syvitski (1992) and Roberts (2001) estimated the total annual sediment load of the lower Mekong River to be 160×10^9 kg yr^{-1} or 150–170 $\times 10^9$ kg yr^{-1}, respectively. However, the discharge fluctuates by several tens of 10^9 kg yr^{-1} on an inter-annual scale (Lu and Siew, 2006) and the estimates are also affected by the measuring technique, which is based on monthly sampling of suspended load just below water surface (Kummu and Varis, 2007) and recent changes due to dam constructions (Kummu et al., 2010; Wang et al., 2011). Moreover, the sediment load may increase even by 10% between the measuring station and the river mouth due to supply from the lower Mekong River catchment (Kummu et al., 2010). For the calculation and comparison with existing values of sediment storage for various parts of the Mekong River dispersal system the commonly cited value of 160×10^9 kg yr^{-1} (Milliman and Syvitski, 1992) is used. This sediment load is distributed over the succession of depositional areas and for each of them a separated budget calculation is provided in the following.

5.3.1. The Tonle Sap Lake

Between Pakse and the Mekong River delta, the river leaves about 3.7×10^9 kg yr^{-1} of sediment in the Tonle Sap Lake in southern Cambodia (Fig. 1B), which thus acts as a sediment trap (Kummu et al., 2008). This lake is connected to the Mekong River through the 120-

km long Tonle Sap River. During the rainy season between May and October the water level in the Mekong River is so high that the water flow direction between the lake and river is reversed allowing Mekong River waters to enter the Tonle Sap Lake and leading to an up to fivefold increase of the lake area (Puy et al., 1999). SARs of mud in the lake are lower than 0.1 cm yr^{-1} on average (Penny et al., 2005). According to modeling by Kummu et al. (2008) about 80% of the lake sediments originate from the Mekong River and total annual mass of sediments left in the Tonle Sap Lake system is estimated to be approximately 2.3% of the total Mekong River sediment load.

5.3.2. The delta plain

Sediment accumulation on the delta plain is related to seasonal floods which lead to inundation of two regions on its northern part: the Long Xuyen Quadrangle in the northwest and the Plain of Reeds in the northeast, covering areas of 5000 and 8000 km^2, respectively (Fig. 9; e.g., Sakamoto et al., 2007; Haruyama, 2011). Hung et al. (in press-a) monitored floodplain sediment deposition rates for three successive years in their study area extending for about 20 km from the main river channel and considered to be representative for these regions. They observed annual accumulation rates in the range between 0.3 and 20 kg m^{-2} with an average of 6.8 kg m^{-2}. These depositional rates are expected to decrease with distance to the Mekong River channels in accordance with observed decrease in suspended sediment concentrations in flooding waters (Hung et al., in press-b). However, since no data exist on the spatial variability of SARs farther from the river in the Long Xuyen Quadrangle and the Plain of Reeds the present calculation assumes arbitrarily that the accumulation is mainly focused in approximately up to 25 km wide belts adjacent to the main river channels (DP in Fig. 9), which overlap with the deep flood inundation area (Haruyama, 2011) and sums up to approximately 6500 km^2. The calculated annual sediment storage on the delta plain using the average annual sediment accumulation of 6.8 kg m^{-2} plain accounts for more than one forth of annual fluvial suspended load (Table 4).

5.3.3. The subaqueous delta platform

The subaqueous delta front comprising platform (SDP) and slope (SDS) is composed mainly of sand next to the river mouths and of mud-dominated sediments in the distal part around the Camau Peninsula (Unverricht et al., 2013–this issue). As the sediment budget calculation focuses on fine-grained sediments, only the western part of the subaqueous delta is taken into account (Fig. 9). The subaqueous delta platform sediments contain at least 60% of mud on average (Unverricht et al., 2013–this issue). SARs on the delta platform are not well constrained. The rate of Camau Peninsula progradation (26 m yr^{-1}) as well as available seismic reflection data (Xue et al., 2010; Unverricht, unpublished data) suggest that the delta platform is an active depocenter. The SAR of 0.5 cm yr^{-1} is assumed here for calculations. The bulk density of the sediments of the subaqueous delta as well as of the continental shelf deposits is applied from the relation of grain-size to density in comparable environments (for instance by Shi et al., 2003) confirmed by few own assessments based on sediment core samples taken from known sediment volume and weight. Applying a dry bulk density of 1 kg m^3 and the area of 2500 km^2 the annual mass of stored fine-grained sediments is about 7.5×10^9 kg (Table 4).

5.3.4. The subaqueous delta slope

The highest SARs in the Mekong River delta system are documented for eleven sediment cores using ^{210}Pb and ^{137}Cs (Fig. 9) (Xue et al., 2010, in press; Unverricht et al., 2013–this issue) in the subaqueous delta slope region. The reported values range between >2.5 cm yr^{-1} and >10 cm yr^{-1} (Fig. 9). In many cores it was possible only to assess that the accumulation is rapid (excess ^{210}Pb was present throughout the cores) and to estimate minimum SARs. For the calculations a value of 5 cm yr^{-1} was arbitrarily taken as an average SAR. The average mud content is 70%, although it is important to underline that the sediment composition is rather heterogeneous (Unverricht et al., 2013–this issue). Applying a dry bulk density of 1 kg m^3 and the area of 2800 km^2 the annual mass of fine-grained sediments is about 98×10^9 kg, which is more than a half of the total river suspended load (Table 4).

5.3.5. The subaqueous prodelta

The next environment included in the budget calculation is part of the Zone A dominated by mud and sandy mud (Fig. 2), interpreted as the prodelta (Fig. 9). The modern SAR is estimated to be 0.5 cm yr^{-1} using the dating results from three cores of the present study and one from Xue et al. (2010). The dry bulk density was assumed to be 1.2 kg m^3 and the calculated annual mass of mud fraction deposited in this area is 41.3×10^9 kg, which is approximately one fourth of total river sediment discharge (Table 4).

5.3.6. The open shelf

The open-shelf area (Zone C) is dominated by sands. Only the part surrounding the subaqueous prodelta off the Camau Peninsula which is covered with muddy sand is considered here as a sink for Mekong River fine-grained sediments (Fig. 9). The SAR based on the presented results (two cores) is assessed to be 0.3 cm yr^{-1}. The bulk density was assumed to be 1.5 kg m^3 and the calculated amount of annually accumulating mud is 6.3×10^9 kg which is approximately 4% of total river sediment discharge (Table 4).

5.3.7. Limitations and implications of the sediment budget

The calculated budget reveals that probably the subaqueous delta front (platform and slope) sequestrates about 50% of the supplied fine-grained sediments with roughly 25% of sediment stored on the terrestrial part of the delta (including the Tonle Sap Lake) and on the shelf around the Camau Peninsula (mainly within prodelta deposits), respectively. This first order sediment budget estimate for the modern fine-grained material has to consider many assumptions. The total mass of sediments stored annually in the various depocenters of the onshore-

Table 4
Modern fine-grained sediment budget for the Mekong River sediments. See text (Section 5.3) for a discussion and explanations and Fig. 9B for location. Areas used for calculations are marked in Fig. 9 (for DP, SD, ZA and ZC). Mud fraction is expressed as 0 (0%) to 1 (100%). Total sediment mass accumulated in particular regions is calculated by multiplying average mass accumulation rate, area and mud fraction. The percent of the total river sediment discharge is calculated by dividing the total mass by 160×10^9 kg yr^{-1}. Note that the sum of the sediment masses in the accumulation regions is over 100%. Data sources: 1) Milliman and Syvitski (1992), 2) Roberts (2001), 3) Penny et al. (2005), 4) Kummu et al. (2008), 5) Hung et al. (in press-a), 6) Xue et al. (2010), 7) Xue et al. (in press), 8) Unverricht et al. (2013–this issue), 9) current paper.

Accumulation region	Average mass accumulation rate (kg m^{-2})	Area (km^2)	Mud fraction	Total mass (10^9 kg yr^{-1})	% of river discharge (160×10^9 kg yr^{-1})	Data source
Mekong River Discharge (RD)	–	–	1	150–170	—	1, 2
Tonle Sap Lake (TS)	0.9	10,000	1	3.7	2.3%	3, 4
Mekong Delta Plain (DP)	6.8	6500	1	44.2	27.6%	5
Subaqueous Mekong Delta Platform (SDP)	5.5	2500	0.6	7.5	4.7%	6, 7, 8
Subaqueous Mekong Delta Slope (SDS)	50	2800	0.7	98	61.3%	6, 7, 8
Continental shelf adjacent to the delta (*prodelta*) — Zone A (ZA)	6.5	12,500	0.55	41.3	25.8%	9
Continental shelf adjacent to the delta (*offshore*) — Zone C (ZC)	4.5	7000	0.2	6.3	3.9%	9
Total					125.6%	

offshore deltaic system (~200 × 10^9 kg yr^{-1}) is by approximately 25% greater than the average annual sediment discharge from the river (Table 4). The largest uncertainty in this budget calculation is related to the area of deposition on the delta plain and in the prodelta and with SARs on subaqueous delta. For instance, assuming the average SAR on the subaqueous delta slope to be more or less by 1 cm yr^{-1}, what is not unlikely, would result in the change of the calculated sediment storage by more than 10% of the annual river sediment discharge. The existing data, however, does not allow assessing the uncertainty. Moreover, the calculations of the sediment budget did not include some areas, where potentially some minor amounts of Mekong-River derived fine-grained sediments may be stored (delta front in front of the river mouths, shelf area of Zone B).

A previous Late Holocene sediment budget estimate for the Mekong River delta by Ta et al. (2002b) and Xue et al. (2010) based on deltaic sediment thickness and progradation rate during the past 3000 yr came up with a conclusion that ~80% of the sediments delivered by the Mekong River is stored in prograding delta. However, these estimations do include storage on lower delta plain, subaqueous delta and prodelta, as all of these sedimentary facies were documented in the sediment cores used for the assessment of the sediment thickness (Ta et al., 2002a,b). These estimates did not include the sediment accumulation on flood plains in the northern part of the delta and on Plain of Reeds assessed to be approximately 1 to 6.7 m ka^{-1} (Tamura et al., 2009) and 0.1 to 0.3 m ka^{-1} (Hanebuth et al., 2012), respectively.

Both, modern and Late Holocene sediment budget calculations show that likely almost all of the fine-grained sediments transported by the Mekong River system are sequestrated either in the deltaic system itself or on the adjacent continental shelf, mainly westward from the modern Mekong River mouths. Consequently, the sediment export toward the deep South China Sea is probably negligible and other sources of terrigenous sediments should be also considered while interpreting deep sea sedimentary record for Late Holocene but probably also for all the sea level highstand intervals. For instance, minor short rivers draining the mountains of central Vietnam deliver annually up to 40 × 10^9 kg yr^{-1} of sediments to the ocean (Thanh et al., 2004) and large part of this material is probably transferred across the narrow Vietnamese continental shelf into the open ocean as discussed by Schimanski and Stattegger (2005) and Szczuciński et al. (2009).

6. Conclusions

The current study shows that well-developed mud-rich prodelta extends westward next to the subaqueous delta front of the Camau Peninsula and is detached from the delta front off of the Mekong River mouths. The combination of sedimentological, mineralogical and geochemical investigations allowed us to distinguish three major zones dominated by muddy deposits (prodelta), terrigenous sands (inner shelf) and carbonate sands and gravels (outer shelf). The clay-mineral composition suggests that the fine-grained portion of these sediments is primarily derived from the Mekong River, except in the northeastern region where local sources seem to contribute as well. Sediments in each of these zones are subject to redeposition processes likely related to episodic tropical storm events and are affected in shallower parts by tides, monsoonal wind waves and coastal currents. A simple sediment budget calculation reveals that the subaqueous delta front stores about 50% of fine-grained sediments supplied by the Mekong River. Roughly 25% of the sediments are retained in the subaerial part of the delta and another 25% accumulate on the shelf around the Camau Peninsula mainly in the form of prodelta deposits. These results contradict assumptions of a significant export of fine-grained sediments into the deep South China Sea basin.

Although the current study provides basic contributions to the understanding of the Mekong River offshore sediment dispersal system, several questions remain open for future studies. For instance, the three defined zones (A, B, C) exhibit open boundaries, and the extent to which the Mekong River subaqueous prodelta is extending to the far west is particularly intriguing. The sedimentary structures and ^{210}Pb activity profiles reveal complex sedimentary processes with event deposition and frequent erosion and redeposition. However, a better understanding of the driving processes behind this process, and particularly of the local hydrodynamics that include in-situ measurements, is required to assess the importance of particular processes. Finally, the sediment budget for the Mekong River depositional system presented here is a first-order approximation and does not include the bed-load transport component, which is certainly an important part of the total river discharge.

Acknowledgments

Funds for this study were provided by the Polish National Committee on Scientific Research (KBN) grant no. 6 PO4D 051 30, the German Federal Ministry of Education and Research (BMBF) grant nos. 03G0140A and B and DFG project *Land–Ocean–Atmosphere Interactions in the Coastal Zone of Vietnam* (grant no. STA401/10). Andreas Wetzel was supported by the Swiss National Science Foundation (grant nos. 200021-112128 and 200020_140217/1). We would like to thank Radosław Jagodziński and Michał Kubiak for their help in analytical work and to all cruise participants for onboard collaboration. We also thank the two anonymous reviewers for their constructive comments.

Appendix A. Supplementary data

Supplementary data associated with this article can be found in the online version, at http://dx.doi.org/10.1016/j.gloplacha.2013.08.019. These data include Google maps of the most important areas described in this article.

References

Anikiev, V.V., Zaytsev, O.V., Hieu, T.T., Savil'yeva, I.I., Starodubtsev, Y.G., Shumilin, Y.N., 1986. Variation in the space–time distribution of suspended matter in the coastal zone of the Mekong River. Okeanologiya 26, 259–266.

Anikiev, V.V., Botsul, A.I., Dudarev, O.V., Kolesov, G.M., Sapozhnikov, D.Yu., Shumilin, E.N., 2001. Distribution, fractionation and fluxes of the rare-earth elements in the suspended matter-bottom sediment system in the Mekong and Saigon river estuaries, South China Sea. Geochem. Int. 39, 897–907.

Anikiev, V.V., Shumilin, E.N., Dudarev, O.V., Botsul, A.I., Zakharova, P.V., Kolesov, G.M., Sapozhnikov, D.Y., Smith, R., 2004. Spatial variability in distribution of lithological characteristics and chemical elements in the bottom sediments of the South China Sea near Mekong and Saigon River deltas. Geochem. Int. 42, 1154–1171.

Aoki, S., 1976. Clay mineral distribution in sediments of the Gulf of Thailand and the South China Sea. J. Oceanogr. Soc. Jpn. 32, 169–174.

Astakhov, A.S., Markov, Yu.L., Ching, T.H., 1989. Influence of Mekong River on late Quaternary sedimentation in South China sea. [in Russian] Litol. Pol. Iskop. 3, 112–127.

Biscaye, P.E., 1965. Mineralogy and sedimentation of recent deep-sea clay in the Atlantic Ocean and adjacent seas and oceans. Geol. Soc. Am. Bull. 76, 803–832.

Bui, V.D., Schimanski, A., Stattegger, K., Phung, V.P., Nguyen, T.T., Nguyen, T.H., Nguyen, T.T., Phi, T.T., 2009. Sandwaves on the Southeast Vietnam Shelf recorded by high resolution seismic profiles: formation and mechanism. Front. Earth Sci. China 3, 9–20.

Cenci, R.M., Martin, J.M., 2004. Concentration and fate of trace metals in Mekong River Delta. Sci. Total. Environ. 332, 167–182.

Chen, P.Y., 1978. Minerals in bottom sediments of the South China Sea. Geol. Soc. Am. Bull. 89, 211–222.

Cohen, S., Kettner, A.J., Syvitski, J.P.M., Fekete, B.M., 2013. WBMsed, a distributed global-scale riverine sediment flux model: model description and validation. Comput. Geosci. 53, 80–93.

Coleman, J.M., Roberts, H.H., 1989. Deltaic coastal wetlands. Geol. Mijnb. 68, 1–24.

Conley, D.J., 1997. Riverine contribution of biogenic silica to the oceanic silica budget. Limnol. Oceanogr. 42, 774–777.

Emery, K.O., 1968. Relict sediments on continental shelves of world. Am. Assoc. Pet. Geol. Bull. 74, 541–554.

Emery, K.O., Nino, H., 1963. Sediments of the Gulf of Thailand and adjacent continental shelf. Geol. Soc. Am. Bull. 74, 541–554.

Fang, G., Kwok, Y.-K., Yu, K., Zhu, Y., 1999. Numerical simulation of principal tidal constituents in the South China Sea, Gulf of Tonkin and Gulf of Thailand. Cont. Shelf Res. 19, 845–869.

Folk, R.L., 1954. The distinction between grain size and mineral composition in sedimentary rock nomenclature. J. Geol. 62, 344–359.

Fu, S., Zhu, Z., Ouyang, T., Qiu, Y., Wei, Z., 2011. Geochemical changes of the terrigenous sediments in the southern South China Sea and their paleoenvironmental implications during the last 31 ky. J. Oceanogr. 67, 337–346.

Gagliano, S.M., McIntire, W.G., 1968. Reports on the Mekong River Delta. Technical Report, 57. Coastal Studies Institute, Louisiana State University, p. 144.
Gingele, F.X., Deckker, P.D., Hillenbrand, C.D., 2001. Clay mineral distribution in surface sediments between Indonesia and NW Australia: source and transport by current oceans. Mar. Geol. 179, 135–146.
Goodbred Jr., S.L., Kuehl, S.A., 1999. Holocene and modern sediment budgets for the Ganges–Brahmaputra river system: evidence for highstand dispersal to flood-plain, shelf, and deep-sea depocenters. Geology 27, 559–562.
Goodbred Jr., S.L., Saito, Y., 2012. Tide-dominated deltas. In: Davis, R.A., Dalrymple, R.W. (Eds.), Principles of Tidal Sedimentology. Springer Science + Business Media B.V, pp. 129–149.
Govindaraju, K., 1994. Compilation of working values and sample description for 383 geostandards. Geostand. Newslett. 18, 1–158.
Hanebuth, T.J.J., Stattegger, K., 2004. Depositional sequences on a late Pleistocene–Holocene tropical siliciclastic shelf (Sunda Shelf, southeast Asia). J. Asian Earth Sci. 23, 113–126.
Hanebuth, T., Stattegger, K., Bojanowski, A., 2009. Termination of the Last Glacial Maximum sea-level lowstand: the Sunda-Shelf data revisited. Glob. Planet. Change 66, 76–84.
Hanebuth, T.J.J., Voris, H.K., Yokoyama, Y., Saito, Y., Okuno, J., 2011. Formation and fate of sedimentary depocentres on Southeast Asia's Sunda Shelf over the past sea-level cycle and biogeographic implications. Earth Sci. Rev. 104, 92–110.
Hanebuth, T.J.J., Proske, U., Saito, Y., Nguyen, V.L., Tac, T.K.O., 2012. Early growth stage of a large delta — transformation from estuarine-platform to deltaic-progradational conditions (the northeastern Mekong River Delta, Vietnam). Sediment. Geol. 261–262, 108–119.
Haruyama, S., 2011. Land use and fluvial geomorphology of the lower Mekong delta in Vietnamese territories — lesson from local knowledge of the land use for future regional planning based on geomorphologic features. In: Haruyama, S. (Ed.), Human and Natural Environmental Impact for the Mekong River, TERRAPUB, Tokyo, pp. 167–195.
Hay, W.W., 1998. Detrital sediment fluxes from continents to oceans. Chem. Geol. 145, 287–323.
Hieu, T.T., 1998. The bottom sediments in the south-west marine region of Vietnam. Contrib. Mar. Geol. Geophys. 4, 156–163.
Hordoir, R., Nguyen, K.D., Polcher, J., 2006. Simulating tropical river plumes, a set of parametrizations based on macroscale data: a test case in the Mekong Delta region. J. Geophys. Res. 111, C09036. http://dx.doi.org/10.1029/2005JC003392.
Hori, K., Saito, Y., 2007. Classification, architecture, and evolution of large-river deltas. In: Gupta, A. (Ed.), Large Rivers: Geomorphology and Management. John Wiley & Sons Ltd., pp. 75–96.
Hung, N.N., Delgado, J.M., Günter, A., Merz, B., Bárdossy, A., Apel, H., 2013. Sedimentation in the floodplains of the Mekong Delta, Vietnam. Part II: deposition and erosion. Hydrol. Processes. http://dx.doi.org/10.1002/hyp.9855 (in press).
Hung, N.N., Delgado, J.M., Günter, A., Merz, B., Bárdossy, A., Apel, H., 2013. Sedimentation in the floodplains of the Mekong Delta, Vietnam. Part I: suspended sediment dynamics. Hydrol. Processes. http://dx.doi.org/10.1002/hyp.9856 (in press).
Jagodziński, R., 2005. Petrography and Geochemistry of Surface Sediments from Sunda and Vietnamese Shelves (South China Sea). Adam Mickiewicz University Press, Poznań (144 pp.).
Kirchner, G., 2011. ^{210}Pb as a tool for establishing sediment chronologies: examples of potentials and limitations of conventional dating models. J. Environ. Radioact. 102, 490–494.
Kubicki, A., 2008. Large and very large subaqueous dunes on the continental shelf off southern Vietnam, South China Sea. Geo-Mar. Lett. 28, 229–238.
Kuehl, S.A., Nittrouer, C.A., DeMaster, D.J., Curtin, T.B., 1985. An overview of sedimentation on the Amazon continental shelf. Geo-Mar. Lett. 4, 207–210.
Kummu, M., Varis, O., 2007. Sediment-related impacts due to upstream reservoir trapping, the Lower Mekong River. Geomorphology 85, 275–293.
Kummu, M., Penny, D., Sarkkula, J., Koponen, J., 2008. Sediment—curse or blessing for Tonle Sap Lake? Ambio 37, 158–163.
Kummu, M., Lu, X.X., Wang, J.J., Varis, O., 2010. Basin-wide sediment trapping efficiency of emerging reservoirs along the Mekong. Geomorphology 119, 181–197.
Le, T.V.H., Nguyen, H.N., Wolanski, E., Tran, T.C., Haruyama, S., 2007. The combined impact on the flooding in Vietnam's Mekong River delta of local man-made structures, sea level rise, and dams upstream in the river catchment. Estuar. Coast. Shelf Sci. 71, 110–116.
Leslie, C., Hancock, G.J., 2008. Estimating the date corresponding to the horizon of the first detection of 137Cs and 239 + 240Pu in sediment cores. J. Environ. Radioact. 99, 483–490.
Liu, Z., Trentesaux, A., Clemens, S.C., Colin, C., Wang, P., Huang, B., Boulay, S., 2003. Clay mineral assemblages in the northern South China Sea: implications for the East Asian monsoon evolution over the past 2 million years. Mar. Geol. 201, 133–146.
Liu, Z., Colin, C., Trentesaux, A., Blamart, D., Bassinot, F., Siani, G., Sicre, M.A., 2004. Erosional history of the eastern Tibetan Plateau since 190 kyr ago: clay mineralogical and geochemical investigations from the southwestern South China Sea. Mar. Geol. 209, 1–18.
Liu, Z., Colin, C., Huang, W., Phon Le, K., Tong, S., Chen, Z., Trentesaux, A., 2007. Climatic and tectonic controls on weathering in south China and Indochina Peninsula: clay mineralogical and geochemical investigations from the Pearl, Red, and Mekong drainage basins. Geochem. Geophys. Geosyst. 8, Q05005. http://dx.doi.org/10.1029/2006GC001490.
Liu, J.P., Xue, Z., Ross, K., Wang, H.J., Yang, Z.S., Li, A.C., Gao, S., 2009. Fate of sediments delivered to the sea by Asian large rivers: long-distance transport and formation of remote alongshore clinothems. Sediment. Rec. 7, 4–9.
Lu, X.X., Siew, R.Y., 2006. Water discharge and sediment flux changes over the past decades in the Lower Mekong River: possible impacts of the Chinese dams. Hydrol. Earth Syst. Sci. Discuss. 10, 181–195.
McKee, B.A., Nittrouer, C.A., DeMaster, D.J., 1983. Concepts of sediment deposition and accumulation applied to the continental shelf near the mouth of the Yangtze River. Geology 11, 631–633.
Michels, K.H., Kudrass, H.R., Hubscher, C., Suckow, A., Wiedicke, M., 1998. The submarine delta of the Ganges–Brahmaputra: cyclone-dominated sedimentation patterns. Mar. Geol. 149, 133–154.
Milliman, J.D., Meade, R., 1983. World-wide delivery of river sediment to the oceans. J. Geol. 91, 1–21.
Milliman, J.D., Syvitski, J.P., 1992. Geomorphic\tectonic control of sediment discharge to the ocean: the importance of small mountainous rivers. J. Geol. 100, 525–544.
Müller, G., Gastner, M., 1971. The carbonate bomb, a simple device for the determination of carbonate content in the sediments, soils and other materials. N. Jahrb. Mineral. 10, 466–469.
Nguyen, V.T., 1996. Characteristics of Quaternary sediments of the continental shelf in a part of southern Vietnam. (in Vietnamese with English abstract) Contrib. Mar. Geol. Geophys. 2, 200–219.
Nguyen, C.T., 2012. Processes and Factors Controlling and Affecting the Retreat of Mangrove Shorelines in South Vietnam. (PhD thesis) Kiel University, Kiel, Germany 130 (http://eldiss.uni-kiel.de/macau/receive/dissertation_diss_00011050).
Nguyen, V.L., Ta, T.K.O., Tateishi, M., 2000. Late Holocene depositional environments and coastal evolution of the Mekong River Delta, Southern Vietnam. Journal of Asian Earth Sciences 18, 427–439.
Nguyen, V.L., Ta, T.K.O., Saito, Y., 2010. Early Holocene initiation of the Mekong River delta, Vietnam, and the response to Holocene sea-level changes detected from DT1 core analyses. Sediment. Geol. 230, 146–155.
Nittrouer, C.A., DeMaster, D.J., McKee, B.A., Cutshall, N.H., Larson, I.L., 1984. The effect of sediment mixing on ^{210}Pb accumulation rates for the Washington continental shelf. Mar. Geol. 54, 201–221.
Nittrouer, C.A., Austin, J.A., Field, M.E., Kravitz, J.H., Syvitski, J.P.M., Wiberg, P.L. (Eds.), 2007. Continental Margin Sedimentation: From Sediment Transport to Sequence Stratigraphy (Special Publication 37 of the IAS). Blackwell Publishing (560 p.).
Patchineelam, S.M., de Figueiredo, A.G., 2000. Preferential settling of smectite on the Amazon continental shelf. Geo-Mar. Lett. 20, 37–42.
Penny, D., Cook, G., Im, S.S., 2005. Long-term rates of sediment accumulation in the Tonle Sap, Cambodia: a threat to ecosystem health? J. Paleolimnol. 33, 95–103.
Petschik, R., 2000. MacDiff 4.2.5 Manual. [Online]. Available from: http://www.geologie.uni-frankfurt.de/Staff/Homepages/Petschick/RainerE.html.
Porrenga, D.H., 1966. Clay minerals in recent sediments off the Niger Delta. 14th National Conference on, Clays and Clay Minerals, pp. 221–233.
Porrenga, D.H., 1967. Glauconite and chamosite as depth indicators in the marine environment. Mar. Geol. 5, 495–501.
Puy, L., Sovan, L., Touch, S.T., Mao, S.O., Chhouk, B., 1999. Diversity and spatial distribution of freshwater fish in Great Lake and Tonle Sap river (Cambodia, Southeast Asia). Aquat. Living Resour. 12, 379–386.
Robbins, J.A., Edgington, D.N., 1975. Determination of recent sedimentation rates in Lake Michigan using Pb-210 and Cs-137. Geochim. Cosmochim. Acta 39, 285–304.
Roberts, T., 2001. Downstream Ecological Implications of China's Lancang Hydropower and Mekong Navigation Project. International Rivers Network (available at http://www.irn.org/programs/lancang/).
Sakamoto, T., Nguyen, N.V., Kotera, A., Ohno, H., Ishitsuka, N., Yokozawa, M., 2007. Detecting temporal changes in the extent of annual flooding within the Cambodia and the Vietnamese Mekong Delta from MODIS time-series imagery. Remote. Sens. Environ. 109, 295–313.
Schimanski, A., Stattegger, K., 2005. Deglacial and Holocene evolution of the Vietnam Shelf: stratigraphy, sediments and sea-level change. Mar. Geol. 214, 365–387.
Shi, C., Zhang, D.D., You, L., 2003. Sediment budget of the Yellow River delta, China: the importance of dry bulk density and implications to understanding of sediment dispersal. Mar. Geol. 199, 13–25.
Smith, J.N., 2001. Why should we believe ^{210}Pb sediment geochronologies? J. Environ. Radioact. 55, 121–123.
Sommerfield, C.K., Ogston, A.S., Mullenbach, B.L., Drake, D.E., Alexander, C.R., Nittrouer, C.A., Borgeld, J.C., Wheatcroft, R.A., Leithold, E.L., 2007. Oceanic dispersal and accumulation of river sediment. In: Nittrouer, C.A., Austin, J.A., Field, M.E., et al. (Eds.), Continental Margin Sedimentation. International Association of Sedimentologists, Special Publication, 37, pp. 157–212.
Steinke, S., Hanebuth, T.J.J., Vogt, C., Stattegger, K., 2008. Sea level variations in clay mineral composition in the southwestern South China Sea over the past 17,000 yr. Mar. Geol. 250, 199–210.
Syvitski, J.P.M., Milliman, J.D., 2007. Geology, geography, and humans battle for dominance over the delivery of fluvial sediment to the coastal ocean. J. Geol. 115, 1–19.
Syvitski, J.P.M., Vörösmarty, C.J., Kettner, A.J., Green, P., 2005. Impact of humans on the flux of terrestrial sediment to the global coastal ocean. Science 308, 376–380.
Syvitski, J.P.M., Kettner, A.J., Overeem, I., Hutton, E.W.H., Hannon, M.T., Brakenridge, G.R., Day, J., Vörösmarty, C., Saito, Y., Giosan, L., Nicholls, R.J., 2009. Sinking deltas due to human activities. Nat. Geosci. 2, 681–686.
Szczuciński, W., Stattegger, K., Scholten, J., 2009. Modern sediments and sediment accumulation rates in a monsoonal narrow shelf setting — central Vietnam, South China Sea. Geo-Mar. Lett. 29, 47–59.
Ta, T.K.O., Nguyen, V.L., Tateishi, M., Kobayashi, I., Saito, Y., Nakamura, T., 2002a. Sediment facies and Late Holocene progradation of the Mekong River Delta in Bentre Province, southern Vietnam: an example of evolution from tide-dominated to a tide- and wave-dominated delta. Sediment. Geol. 152, 313–325.
Ta, T.K.O., Nguyen, V.L., Tateishi, M., Kobayashi, I., Tanabe, S., Saito, Y., 2002b. Holocene delta evolution and sediment discharge of the Mekong River, southern Vietnam. Quat. Sci. Rev. 21, 1807–1819.

Ta, T.K.O., Nguyen, V.L., Tateishi, M., Kobayashi, I., Saito, Y., 2005. Holocene delta evolution and depositional models of the Mekong river delta, southern Vietnam. In: Giosan, L., Bhattacharya, J.P. (Eds.), River Deltas — Concepts, Models, and Examples. SEPM Spec. Publ. no. 83, pp. 453–466.

Tamura, T., Saito, Y., Sieng, S., Ben, B., Kong, M., Sim, I., Choup, S., Akiba, F., 2009. Initiation of the Mekong River delta at 8 ka: evidence from the sedimentary succession in the Cambodian lowland. Quat. Sci. Rev. 28, 327–344.

Tamura, T., Horaguchi, K., Saito, Y., Nguyen, V.L., Tateishi, M., Ta, T.K.O., Nanayama, F., Watanabe, K., 2010. Monsoon-influenced variations in morphology and sediment of a mesotidal beach on the Mekong River Delta coast. Geomorphology 116, 11–23.

Thanh, T.D., Saito, Y., Huy, D.V., Nguyen, V.L., Ta, T.K.O., Tateishi, M., 2004. Regimes of human and climate impacts on coastal changes in Vietnam. Reg. Environ. Change 4, 49–62.

Thiry, M., 2000. Paleoclimatic interpretations of clay minerals in marine deposits: an outlook from the continental origin. Earth Sci. Rev. 49, 201–221.

Tjallingii, R., Stattegger, K., Wetzel, A., Van Pach, P., 2010. Infilling and flooding of the Mekong River incised-valley system during deglacial sea-level rise. Quat. Sci. Rev. 29, 1432–1444.

UNISYS, 2013. http://weather.unisys.com/hurricane/w_pacific/index.php.

Unverricht, D., Nguyen, T.C., Heinrich, C., Szczuciński, W., Lahajnar, N., Stattegger, K., 2013. Suspended sediment dynamics during the inter-monsoon season in the subaqueous Mekong Delta and adjacent shelf, southern Vietnam. J. Asian Earth Sci. http://dx.doi.org/10.1016/j.jseaes.2012.10.008 (in press).

Unverricht, D., Szczuciński, W., Stattegger, K., Jagodziński, R., Le, X.T., Kwong, L.L.W., 2013. Modern sedimentation and morphology of the subaqueous Mekong Delta, Southern Vietnam. Glob. Planet. Change. 110, 223–235 (this issue).

Walsh, J.P., Nittrouer, C.A., 2009. Understanding fine-grained river-sediment dispersal on continental margins. Mar. Geol. 263, 34–45.

Wang, H., Saito, Y., Zhang, Y., Bi, N., Sun, X., Yang, Z., 2011. Recent changes of sediment flux to the western Pacific Ocean from major rivers in East and Southeast Asia. Earth Sci. Rev. 108, 80–100.

Wendong, F., Zhongxin, G., Yuting, H., 1998. Observational study of the circulation in the southern South China Sea. Chin. Sci. Bull. 43, 898–905.

Wetzel, A., 1993. The transfer of river load to deep-sea fans: a quantitative approach. Am. Assoc. Pet. Geol. Bull. 77, 1679–1692.

Wetzel, A., Tjallingii, R., Stattegger, K., 2010. Gyrolithes in Holocene estuarine incised valley fill deposits, offshore southern Vietnam. Palaios 25, 239–246.

Wiesner, M.G., Stattegger, K., Voß, M., Schwarzer, K., Pohlmann, T., Amann, T., Dombar, D., de Silva, L., Dippner, J., Do, H.C., Doan, N.H., Kiem, D.T., Freing, A., Grosse, J., Heidemann, U., Hein, H., Heyckendorf, K., Jagodzinski, R., Kagelmacher, A., Lahajnar, N., Le, X.T., Liskow, I., Moisander, P., Montoya, J., Nguyen, B.M., Nguyen, D.C., Nguyen, H.H., Nguyen, K.V., Nguyen, N.L., Nguyen, T.T., Nguyen, V.T., Peinert, R., Peleo-Alampay, A., Hung, V.P., Schimanski, A., Steen, E., Stochel, T., Subramaniam, A., Szczucinski, W., Tran, V.C., Unverricht, D., Vo, V.L., Welsch, A., Wetzel, A., 2006. Cruise report RV Sonne 187 Vietnam. Land–Ocean–Atmosphere Interactions in the Coastal Zone of Vietnam. Berichte — Reports Institute für Geowissenschaften, 23. Universität Kiel (99 pp.).

Wolanski, E., Huan, N.N., Dao, L.T., Nhan, N.H., Thuy, N.N., 1996. Fine-sediment dynamics in the Mekong River estuary, Vietnam. Estuar. Coast. Shelf Sci. 43, 565–582.

Wright, L.D., Friedrichs, C.T., 2006. Gravity-driven sediment transport on continental shelves: a status report. Cont. Shelf Res. 26, 2092–2107.

Xue, Z., Liu, J.P., DeMaster, D., Nguyen, L.V., Ta, T.K.O., 2010. Late Holocene evolution of the Mekong subaqueous delta, southern Vietnam. Mar. Geol. 269, 46–60.

Xue, Z., He, R., Liu, J.P., Warner, J.C., 2012. Modeling transport and deposition of the Mekong river sediment. Cont. Shelf Res. 37, 66–78.

Xue, Z., Liu, J.P., DeMaster, D., Leithold, E.L., Wan, S., Ge, Q., Nguyen, L.V., Ta, T.K.O., 2013. Sedimentary processes on the Mekong subaqueous delta: clay mineral and geochemical analysis. J. Asian Earth Sci. http://dx.doi.org/10.1016/j.jseaes.2012.07.012 (in press).

Zu, T., Gan, J., Erofeeva, S.Y., 2008. Numerical study of the tide and tidal dynamics in the South China Sea. Deep-Sea Res. I 55, 137–154.